Acknowledgment

This study was supported, in part, by the Grant-in-Aid for Scientific Research (C) from the Japan Society for the Promotion of Science (JSPS).

References

[1] D.H. Adams, A.R. Lloyd, Chemokines: leucocyte recruitment and activation cytokines, Lancet 349 (1997) 490–495.
[2] A.D. Luster, Chemokines–chemotactic cytokines that mediate inflammation, N. Engl. J. Med. 338 (1998) 436–445.
[3] J.M. Wang, X. Deng, W. Gong, S. Su, Chemokines and their role in tumor growth and metastasis, J. Immunol. Methods 220 (1998) 1–17.
[4] A. Muller, B. Homey, H. Soto, N. Ge, D. Catron, M.E. Buchanan, T. McClanahan, E. Murphy, W. Yuan, S.N. Wagner, J.L. Barrera, A. Mohar, E. Verastegui, A. Zlotnik, Involvement of chemokine receptors in breast cancer metastasis, Nature 410 (2001) 50–56.
[5] C.J. Scotton, J.L. Wilson, D. Milliken, G. Stamp, F.R. Balkwill, Epithelial cancer cell migration: a role for chemokine receptors?, Cancer Res. 61 (2001) 4961–4965.
[6] A. Li, M.L. Varney, R.K. Singh, Expression of interleukin 8 and its receptors in human colon carcinoma cells with different metastatic potentials, Clin. Cancer Res. 7 (2001) 3298–3304.
[7] T. Koshiba, R. Hosotani, Y. Miyamoto, J. Ida, S. Tsuji, S. Nakajima, M. Kawaguchi, H. Kobayashi, R. Doi, T. Hori, N. Fujii, M. Imamura, Expression of stromal cell-derived factor 1 and CXCR4 ligand receptor system in pancreatic cancer: a possible role for tumor progression, Clin. Cancer Res. 6 (2000) 3530–3535.
[8] M.M. Robledo, R.A. Bartolome, N. Longo, J.M. Rodriguez-Frade, M. Mellado, I. Longo, G.N. van Muijen, P. Sanchez-Mateos, J. Teixido, Expression of functional chemokine receptors CXCR3 and CXCR4 on human melanoma cells, J. Biol. Chem. 276 (2001) 45098–45105.
[9] M. Miyamoto, Y. Shimizu, K. Okada, Y. Kashii, K. Higuchi, A. Watanabe, Effect of interleukin-8 on production of tumor-associated substances and autocrine growth of human liver and pancreatic cancer cells, Cancer Immunol. Immunother. 47 (1998) 47–57.
[10] K.F. Yoong, S.C. Afford, R. Jones, P. Aujla, S. Qin, K. Price, S.G. Hubscher, D.H. Adams, Expression and function of CXC and CC chemokines in human malignant liver tumors: a role for human monokine induced by gamma-interferon in lymphocyte recruitment to hepatocellular carcinoma, Hepatology 30 (1999) 100–111.
[11] P. Lu, Y. Nakamoto, Y. Nemoto-Sasaki, C. Fujii, H. Wang, M. Hashii, Y. Ohmoto, S. Kaneko, K. Kobayashi, N. Mukaida, Potential interaction between CCR1 and its ligand, CCL3, induced by endogenously produced interleukin-1in human hepatomas, Am. J. Pathol. 162 (2003) 1249–1258.
[12] Y. Itoh, A. Morita, K. Nishioji, H. Fujii, H. Nakamura, T. Kirishima, T. Toyama, N. Yamauchi, Y. Nagao, S. Narumi, T. Okanoue, Time course profile and cell-type-specific production of monokine induced by interferon-gamma in Concanavalin A-induced hepatic injury in mice:comparative study with interferon-inducible protein-10, Scand. J. Gastroenterol. 36 (2001) 1344–1351.
[13] A. Ensser, D. Glykofrydes, H. Niphuis, E.M. Kuhn, B. Rosenwirth, J.L. Heeney, G. Niedobitek, I. Muller-Fleckenstein, B. Fleckenstein, Independence of herpesvirus-induced T cell lymphoma from viral cyclin D homologue, J. Exp. Med. 193 (2001) 637–642.
[14] F. Liao, R. Alderson, J. Su, S.J. Ullrich, B.L. Kreider, J.M. Farber, STRL22 is a receptor for the CC chemokine MIP-3alpha, Biochem. Biophys. Res. Commun. 236 (1997) 212–217.
[15] D.L. Rossi, A.P. Vicari, K. Franz-Bacon, T.K. McClanahan, A. Zlotnik, Identification through bioinformatics of two new macrophage proinflammatory human chemokines: MIP-3alpha and MIP-3beta, J. Immunol. 158 (1997) 1033–1036.
[16] R. Hromas, P.W. Gray, D. Chantry, R. Godiska, M. Krathwohl, K. Fife, G.I. Bell, J. Takeda, S. Aronica, M. Gordon, S. Cooper, H.E. Broxmeyer, M.J. Klemsz, Cloning and characterization of exodus, a novel beta-chemokine, Blood 89 (1997) 3315–3322.
[17] M.C. Dieu, B. Vanbervliet, A. Vicari, J.M. Bridon, E. Oldham, S. Ait-Yahia, F. Briere, A. Zlotnik, S. Lebecque, C. Caux, Selective recruitment of immature and mature dendritic cells by distinct chemokines expressed in different anatomic sites, J. Exp. Med. 188 (1998) 373–386.
[18] B. Homey, M.C. Dieu-Nosjean, A. Wiesenborn, C. Massacrier, J.J. Pin, E. Oldham, D. Catron, M.E. Buchanan, A. Muller, R. deWaal Malefyt, G. Deng, R. Orozco, T. Ruzicka, P. Lehmann, S. Lebecque, C. Caux, A. Zlotnik, Up-regulation of macrophage inflammatory protein-3 alpha/CCL20 and CC chemokine receptor 6 in psoriasis, J. Immunol. 164 (2000) 6621–6632.
[19] J. Kleeff, T. Kusama, D.L. Rossi, T. Ishiwata, H. Maruyama, H. Friess, M.W. Buchler, A. Zlotnik, M. Korc, Detection and localization of Mip-3alpha/LARC/Exodus, a macrophage proinflammatory chemokine, and its CCR6 receptor in human pancreatic cancer, Int. J. Cancer 81 (1999) 650–657.
[20] S.K. Sullivan, D.A. McGrath, F. Liao, S.A. Boehme, J.M. Farber, K.B. Bacon, MIP-3alpha induces human eosinophil migration and activation of the mitogen-activated protein kinases (p42/p44 MAPK), J. Leukoc. Biol. 66 (1999) 674–682.
[21] Y. Sotsios, G.C. Whittaker, J. Westwick, S.G. Ward, The CXC chemokine stromal cell-derived factor activates a Gi-coupled phosphoinositide 3-kinase in T lymphocytes, J. Immunol. 163 (1999) 5954–5963.
[22] R. Seger, E.G. Krebs, The MAPK signaling cascade, FASEB J. 9 (1995) 726–735.
[23] J. Gomez-Cambronero, p42-MAP kinase is activated in EGF-stimulated interphase but not in metaphase-arrested HeLa cells, FEBS Lett. 443 (1999) 126–130.

J Gastroenterol 2004; 39:704–705
DOI 10.1007/s00535-004-1391-0

Journal of Gastroenterology

Editorial

Ribavirin-induced hemolytic anemia in chronic hepatitis C patients

Article on page 668
Factors contributing to ribavirin dose reduction due to anemia during interferon alfa2b and ribavirin combination therapy for chronic hepatitis C
TAKAKI S, TSUBOTA A, HOSAKA T, et al.

In patients with liver diseases, chronic hepatitis C virus (HCV) infection is one of the main causes of predisposition to hepatocellular carcinoma (HCC).[1,2] Since 1992, interferon (IFN)-α and -β have been used to treat chronic hepatitis C (CH-C) patients covered by the public health insurance system in Japan. However, sustained virological response (SVR) was difficult to achieve in CH-C patients with genotype 1b and a high viral load. Recently, the use of ribavirin in combination with IFN has enabled us to achieve a higher SVR rate,[3,4] and peginterferon (PEG-IFN) and rivabirin combination therapy is now being used in Western countries.[5]

Ribavirin is a water-soluble synthetic guanosine analogue which has antiviral as well as immunomodulatory effects. Ning et al.[6] reported that ribavirin modulated the T-helper (Th)1/Th2 balance by inhibiting Th2 cytokine production while preserving Th1 cytokine production. In erythrocytes, ribavirin is converted into mono-, di-, and triphosphorylated intermediates, which cause depletion of adenosine triphosphate and oxidative damage to the erythrocyte membrane, resulting in hemolysis.[7,8]

Although ribavirin-induced hemolytic anemia is reversible, severe anemia during the combination therapy has been reported,[9] and this is one of the most difficult obstacles to be overcome in this current therapy for CH-C. In the drug information for ribavirin, dose reduction is recommended when the hemoglobin (Hb) concentration falls below 10 g/dl, and cessation of ribavirin is requested when the Hb concentration falls below 8.5 g/dl.

Van Vlierbergh et al.[10] investigated the factors influencing the hemolytic anemia occurring during combination therapy for CH-C, using multivariate analysis. They concluded that the pretreatment platelet count, amount of IFN administered, and haptoglobin phenotype were strongly associated with ribavirin-induced hemolytic anemia. In this issue the *Journal of Gastroenterology*, Takaki et al.[11] report their investigation of the factors influencing ribavirin dose reduction due to anemia during the combination therapy in 123 CH-C patients, using univariate analysis. In their report, ribavirin dose reduction was significantly correlated with pretreatment Hb levels (<14 g/dl), female sex, and older age (>55 years), but not with other factors, including platelet count and haptoglobin phenotype. They suggested that more careful monitoring for the Hb level is required in patients before starting the combination therapy, especially those with lower Hb levels and older age. Although they could not clarify the reason for the differences between their results and those reported by Van Vlierbergh et al.,[10] the relatively small number of patients in the study by Takaki et al.[11] or ethnic differences, may account for the differences in results.

To avoid ribavirin-induced hemolytic anemia during the combination therapy, administration of eicosapentaenoic acid (1800 mg/day) was tried, resulting in a significant increase in Hb concentration,[12] while once-weekly administration of erythropoietin (40000 U) was performed by another group,[13] and this succeeded in increasing the Hb concentration, as well as decreasing the dose reduction of ribavirin. Further research in this field is warranted to establish a strategy for effective IFN or PEG-IFN and ribavirin combination therapy for CH-C patients.

Yoshito Itoh, M.D., and Takeshi Okanoue, M.D.
Molecular Gastroenterology and Hepatology, Kyoto Prefectural University of Medicine Graduate School of Medical Science, Kawaramachi-Hirokouji, Kamigyou-ku, Kyoto 602-8566, Japan

Reprint requests to: T. Okanoue

References

1. Tanaka H, Hiyama T, Tsukuma H, Fujimoto I, Yamano H, Okubo Y, et al. Cumulative risk of hepatocellular carcinoma in hepatitis C virus carriers: statistical estimations from cross-sectional data. Jpn J Cancer Res 1994;85:485–90.
2. Shiratori Y, Shiina S, Imamura M, Kato N, Kanai F, Okudaira T, et al. Characteristic difference of hepatocellular carcinoma between hepatitis B and C viral infection in Japan. Hepatology 1995;22:1883–5.
3. McHutchison JG, Gordon SC, Schiff ER, Shiffman ML, Lee WM, Rustgi VK, et al. Interferon alfa-2b alone or in combination with ribavirin as initial treatment for chronic hepatitis C. Hepatitis Interventional Therapy Group. N Engl J Med 1998;339:1485–92.
4. Davis GL, Esteban-Mur R, Rustgi V, Hoefs J, Gordon SC, Trepo C, et al. Interferon alfa-2b alone or in combination with ribavirin for the treatment of relapse of chronic hepatitis C. International Hepatitis Interventional Therapy group. N Engl J Med 1998;339:1493–9.
5. Manns MP, McHutchison JG, Gordon SC, Rustgi VK, Shiffman ML, Reindollar R, et al. Peginterferon alfa-2b plus ribavirin compared with interferon alfa-2b plus ribavirin for initial treatment of chronic hepatitis C: a randomized trial. Lancet 2001;358:958–65.
6. Ning Q, Brown D, Parodo J, Cattral M, Gorczynski R, Cole E, et al. Ribavirin inhibits viral-induced macrophage production of TNF, IL-1, the procoagulant fgl2 prothrombinase and preserves Th1 cytokine production but inhibits Th2 cytokine response. J Immunol 1998;160:3487–93.
7. De Franceschi L, Fattovich G, Turrini F, Ayi K, Brugnara C, Manzato F, et al. Hemolytic anemia induced by ribavirin therapy in patients with chronic hepatitis C virus infection: role of membrane oxidative damage. Hepatology 2000;31:997–1004.
8. Dev A, Patel K, Muir A, McHutchison JG. Erythropoietin for ribavirin-induced anemia in hepatitis C: more answers but many more questions. Am J Gastroenterol 98;2344–7.
9. Tappero G, Ballare M, Farina M, Negro F. Severe anemia following combined alpha-interferon/ribavirin therapy of chronic hepatitis C (letter). Hepatology 1998;29:1033–4.
10. Van Vlierbergh H, Delanghe JR, De Vos M, Leroux-Roel G. BASL steering committee. Factors influencing ribavirin-induced hemolysis. J Hepatol 2001;34:911–6.
11. Takaki S, Tsubota A, Hosaka T, Akuta N, Someya T, Kobayashi M, et al. Factors contributing to ribavirin dose reduction due to anemia during interferon alfa2b and ribavirin combination therapy for chronic hepatitis C. J Gastroenterol 2004;39:668–73.
12. Ide T, Okamura T, Kumashiro R, Koga Y, Hino T, Hisamochi A, et al. A pilot study of eicosapentaenoic acid therapy for ribavirin-related anemia in patients with chronic hepatitis C. Int J Mol Med 2003;11:729–31.
13. Dietrich DT, Wasserman R, Brau N, Hassanein TI, Bini EJ, Bowers PJ, et al. Once-weekly epoetin alfa improves anemia and facilitates maintenance of ribavirin dosing in hepatitis C virus-infected patients receiving ribavirin plus interferon alfa. Am J Gastroenterol 2003;98:2491–9.

ARTICLE

doi:10.1016/j.ymthe.2003.08.005

Engineered Long Terminal Repeats of Retroviral Vectors Enhance Transgene Expression in Hepatocytes *in Vitro* and *in Vivo*

Kanji Yamaguchi,[1,2] Katsuhiko Itoh,[1,*] Naoki Ohnishi,[1] Yoshito Itoh,[2] Christopher Baum,[3] Takashi Tsuji,[4] Toshikazu Nagao,[1] Hiroaki Higashitsuji,[1] Takeshi Okanoue,[2] and Jun Fujita[1]

[1]*Department of Clinical Molecular Biology, Faculty of Medicine, Kyoto University, Kyoto 606-8507, Japan*
[2]*Molecular Gastroenterology and Hepatology, Kyoto Prefectural University of Medicine, Graduate School of Medicine, Kyoto 602-0824, Japan*
[3]*Department of Hematology/Oncology, Hannover Medical School, 30625 Hannover, Germany*
[4]*Department of Applied Biological Science, Faculty of Science and Technology, Tokyo University of Science, Noda 278-8510, Japan*

**To whom correspondence and reprint requests should be addressed at the Department of Clinical Molecular Biology, Faculty of Medicine, Kyoto University, Shogoin-Kawaharacho 54, Sakyo, Kyoto 606-8507, Japan. Fax: +81-75-751-3750. E-mail: katsu@virus.kyoto-u.ac.jp.*

To analyze the important elements for retroviral expression in hepatocytes, *cis*-acting elements in the U3 region of the long terminal repeat (LTR) of the polycythemic strain of spleen focus-forming virus (SFFVp) were analyzed in a hepatocellular carcinoma cell line. Two *cis*-acting elements located within the upstream region of the direct repeat, which positively regulated retroviral expression, were identified. Transcription factors NFAT5 and Sp1, which are ubiquitously expressed in a variety of tissues, bound to these elements. To increase specificity without lowering the potency of retroviral expression in hepatocytes, these elements were replaced by a sequence derived from the hepatitis B virus enhancer II region. Novel vectors, SF-Hep3 and SF-Hep5 (SFFVp-based vector for hepatocytes 3 and 5), were developed with these engineered LTRs. The engineered LTRs of these vectors enhanced the retroviral expression only in hepatocellular carcinoma cell lines *in vitro*. These vectors also increased transgene expression 4- to 9-fold or 3.5- to 5-fold in comparison with a Moloney murine leukemia virus-based vector or a vector containing the wild-type LTR of SFFVp, respectively, in murine hepatocytes *in vivo*.

Key Words: hepatocyte, liver, retrovirus, vector, SFFV, LTR

INTRODUCTION

Retroviral vectors are the most commonly used vehicles for stable gene transfer into various cell types. These vectors can integrate into the host genome to provide long-term transgene expression in the target cells [1,2]. Hepatocytes are attractive targets for these vectors, since they synthesize a myriad of proteins that play pivotal roles in metabolism or hemostasis. One of the major limitations to the use of retroviral vectors in hepatocytes is the low level of transgene expression [3,4].

cis-acting elements located in the U3 region of the retroviral long terminal repeats (LTRs) determine mainly the transcriptional level of newly introduced genes in target cells. Most of the *cis*-acting elements are found within the direct repeat (DR) [5–10]. In addition to in the DR, the elements were also identified in the upstream control region (UCR; the upstream region of the DR) [11–14]. Although these elements were proven to regulate retroviral expression, the activities of these elements have been analyzed in detail mainly in hematopoietic or embryonic cells and not in hepatocytes.

The polycythemic strain of spleen focus-forming virus (SFFVp) is a replication-incompetent virus related to Friend mink cell focus-forming viruses [15]. Its LTR provides high transgene expression in primitive hematopoietic cells [16,17] and spermatogenic cells [18]. Recently, we have demonstrated that the SFFVp U3 also provides about fourfold stronger retroviral enhancer activity than that of the Moloney murine leukemia virus (MoMLV) in hepatocytes *in vivo* [19]. In the present study, we have analyzed the regulatory elements of the SFFVp LTR in a hepatocellular carcinoma cell line and an attempt has been made to enhance its promoter activity especially in hepatocytes.

RESULTS AND DISCUSSION

Strong *cis*-Acting Elements Are Located in the Upstream Region of the DR in SFFVp

To localize the region important for high retroviral expression within the SFFVp U3, we constructed a series of reporter gene plasmids containing the sequence from the

1525-0016/03 $30.00

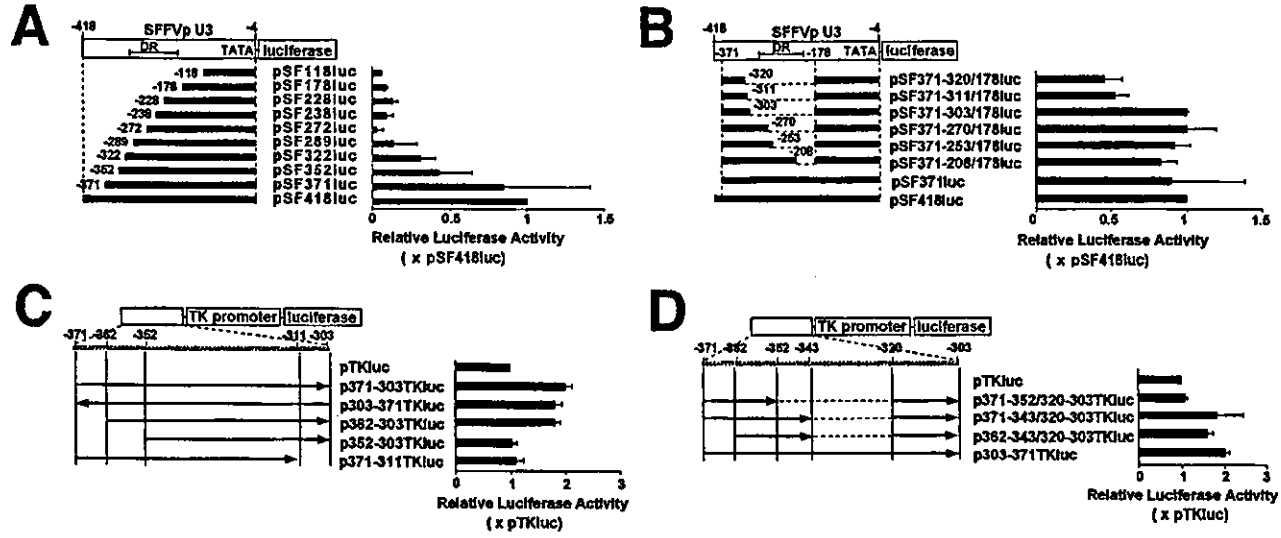

FIG. 1. Transient reporter gene assays of plasmids containing truncated sequences of the SFFVp U3. These plasmids were transfected into PLC/PRF/5 cells. Each column and bar represents the mean value and standard deviation of three assays, respectively. (A) Transient expression of luciferase mediated by the constructs containing a series of 5′ to 3′ truncated sequences of the SFFVp U3. (B) Transient expression of luciferase mediated by the constructs containing a series of 3′ to 5′ truncated sequences of the SFFVp U3. (C, D) Transient expression of luciferase mediated by the constructs containing parts of the UCR and a thymidine kinase promoter.

SFFVp U3 (Fig. 1A). We used a well-differentiated human hepatocellular carcinoma cell line, PLC/PRF/5 [20], for transient reporter assays, since the results of reporter assays in cultured PLC/PRF/5 cells correlated well with those in hepatocytes *in vivo* [19]. pSF418luc contains the sequence from position −4 (4 bp upstream of the cap site) to −418. Deletion of more than 56 bp from the 5′ end significantly reduced the activities (pSF352luc, pSF322luc, or pSF289luc in Fig. 1A), indicating the presence of *cis*-acting elements in the upstream region of the DR (the UCR). We constructed another series of reporter gene plasmids, which contain a series of 3′ to 5′ deletions from position −178 (Fig. 1B). Deletion of the UCR (the region between −371 and −303) reduced the activities to half of that of pSF418luc (pSF371-311/178luc or pSF371-320/178luc in Fig. 1B), confirming the enhancer activity in the UCR.

To analyze the important elements, we cloned the fragment of the U3 from position −371 to −303 into another reporter gene plasmid, pTKluc, containing a thymidine kinase promoter of the herpes simplex virus. This fragment showed enhancer activity regardless of orientation (Fig. 1C, p371-303TKluc and p303-371TKluc). Further analysis showed that the sequences from −362 to −343 and from −320 to −303 were sufficient to enhance the activity (Fig. 1D).

Taken together, these results clarified the enhancer activity of the UCR in SFFVp U3 and that the activity was localized to two regions, spanning from −362 to −343 and from −320 to −303.

Deletion of the Enhancer Elements from Retroviral Vectors Reduces Transgene Expression

To test whether these regions are also crucial for retroviral expression after integration into the genome, we generated a series of retroviral vectors that carry a chloramphenicol acetyltransferase (CAT) gene as a reporter. We produced retrovirus vectors using Phoenix-ampho cells and infected PLC/PRF/5 cells with these vectors. We selected cells in the presence of G418 and measured expression of CAT protein. Although the average numbers of proviral DNAs of SF/CATwt, SF/CATΔ362-343, SF/CATΔ320-303, and SF/CATΔ362-343/320-303 in the pooled cells were not significantly different (1.29, 1.27, 1.25, and 1.46, respectively), the expression levels from the enhancer-deleted vectors (SF/CATΔ362-343, SF/CATΔ320-303, and SF/CATΔ362-343/320-303) were almost equal to one another and were about half of that from SF/CATwt, which contains the full-length LTR (Fig. 2B). These results confirmed the importance of these two regions for retroviral expression.

Mutation Analysis of the *cis*-Regulatory Elements in the UCR

We performed substitution mutation analysis to identify important regulatory elements. We scanned the regions from −362 to −343 and from −320 to −303 using a series of reporter gene plasmids, pMut/1 to pMut/10 (Fig. 3A). Luciferase activities were significantly reduced by the mutation within the region from −358 to −347 or from −313 to −306, while no significant effect was observed

doi:10.1016/j.ymthe.2003.08.005

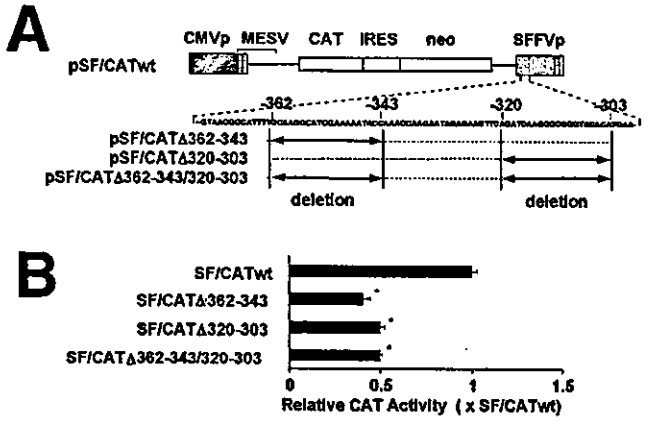

FIG. 2. Expression of the CAT reporter gene in PLC/PRF/5 cells transduced by retroviral vectors containing the truncated UCR. (A) Retroviral vector plasmids containing the deletion within the UCR are schematically shown. (B) Retroviral vector plasmids were transiently transfected into Phoenix-ampho cells and the supernatants were used to transduce PLC/PRF/5 cells. After selection, concentration of CAT protein was measured. Each column and bar represents the mean value and standard deviation of three assays, respectively. *Significantly different from the CAT value mediated by the SF/CATwt vector ($P < 0.005$).

with the flanking mutations (Fig. 3A), indicating that the sequences of GGCATGGAAAAA and GGGCGGGT were crucial for the *cis* activity.

The first sequence, GGCATGGAAAAA, is well conserved among murine retroviruses and is located in the 3′ flanking region of the binding motif for YY-1 (Fig. 3B). The other sequence, GGGCGGGT, is located in the 5′ flanking site of the DR, overlapping the Sp1 binding site [11], and is not conserved between viruses (Fig. 3B).

We have identified these elements located in the UCR and these elements have been proved to be crucial for retroviral expression. On the other hand, there might be some other elements located in regions other than the UCR (i.e., the DR or the 3′ flanking region of the DR) that are also crucial for retroviral expression. Such elements remain to be clarified for our further understanding of high promoter activity of the SFFVp LTR in hepatocytes.

The Nuclear Factor of Activated T Cells 5 (NFAT5) Transcription Factor Binds to the UCR and Enhances Reporter Gene Expression

One of the identified regions (the position from −358 to −347) contains the GGA core motif for NFAT [21] and the substitution mutation analysis showed a clear preference for the sequence longer than the core motif, which contains the target motif for NFAT5 (PuTGGAAAnA) [24]. Since the expression of NFAT5, but not NFAT1, NFAT2, nor NFAT3, was detected by RT-PCR in PLC/PRF/5 cells (data not shown), we analyzed the binding ability of NFAT5 to this region. We transfected pCMV/flag-NFAT5, which contains human NFAT5 cDNA tagged by flag sequences (Fig. 4A), into HEK293T cells and used nuclear extracts for electrophoretic mobility shift assays. One of

FIG. 3. Substitution mutation analysis of the *cis*-regulatory elements. (A) Transient expression of luciferase mediated by the constructs containing three to four base pair substitution mutations. Each column and bar represents the mean value and standard deviation of three assays, respectively. *Significantly different from the value mediated by p362-343/320-303TKluc ($P < 0.05$). (B) Comparison of the sequences of the upstream region of the DR among murine retroviruses and summary of the mutation analysis. Boxed regions have been identified as crucial *cis*-regulatory sequences in the present study. Doubled underlines indicate the motifs for YY-1, ELP, or Sp1. Dotted sequences are different from the sequences of MoMLV.

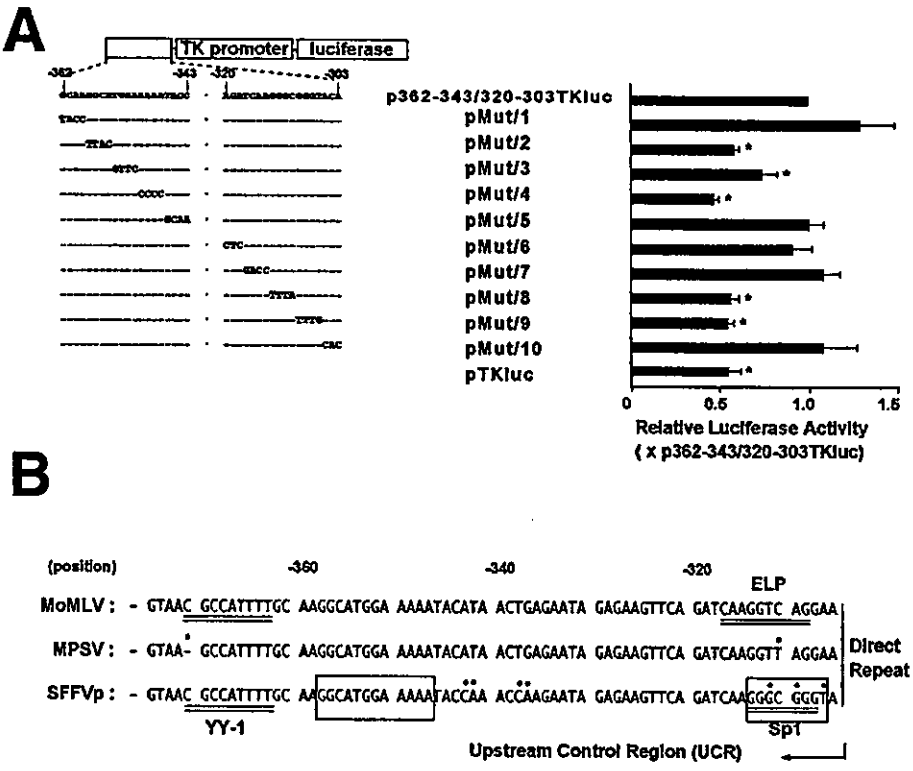

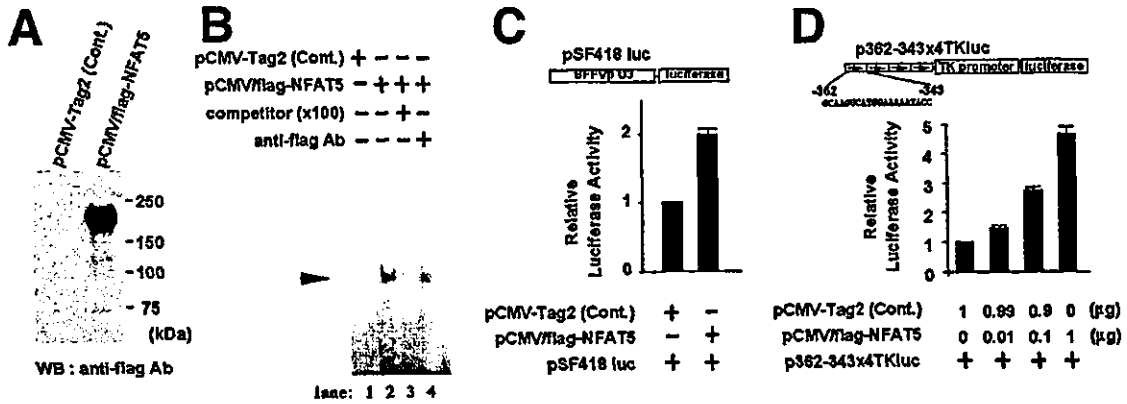

FIG. 4. NFAT5 binds to the UCR and enhances expression. (A) Expression of NFAT5. An expression vector plasmid, pCMV/flag-NFAT5, was transfected into HEK293T cells. Cell lysate was analyzed by Western blotting using an antibody to flag. (B) NFAT5 binds to the UCR. Nuclear extracts from HEK293T cells transfected with pCMV/flag-NFAT5 were analyzed by a gel mobility shift assay. An arrowhead indicates the band detected with oligonucleotides (GGCATG-GAAAAA). The band was abolished or supershifted and diminished by adding 100-times excess of unlabeled oligonucleotides or an anti-flag antibody, respectively. (C) Effects of NFAT5 on luciferase expression mediated by the constructs containing the SFFVp U3. An expression vector plasmid, pCMV/flag-NFAT5, was transfected into HEK293T cells with pSF418luc. Each column and bar represents the mean value and standard deviation of three assays, respectively. (D) Effects of NFAT5 on luciferase expression mediated by the constructs containing four repeats of the sequence corresponding to the position −362 to −343. An expression vector plasmid, pCMV/flag-NFAT5, was transfected into HEK293T cells with p362-343x4TKluc. Each column and bar represents the mean value and standard deviation of three assays, respectively.

the bands detected with oligonucleotides (GGCATG-GAAAAA) (Fig. 4B, lane 2; indicated by an arrowhead) was abolished (lane 3) or supershifted and diminished (lane 4) by adding 100-times excess of unlabeled oligonucleotides or anti-flag antibody, respectively, indicating that NFAT5 protein bound to this sequence.

Next, we examined whether the exogenously expressed NFAT5 increased the expression of a reporter gene. Expression of NFAT5 increased the promoter activity of the SFFVp U3 in HEK293T cells (Fig. 4C). Another reporter plasmid, p362-343x4TKluc, which contained four repeats of the sequence corresponding to position −362 to −343, was also transfected with pCMV/flag-NFAT5 (Fig. 4D). The transfection of pCMV/flag-NFAT5 increased the luciferase activity in a dose-dependent manner, indicating that NFAT5 could enhance the retroviral expression.

NFAT5 belongs to the NFAT family of transcription factors and has also been designated as a tonicity enhancer binding protein, TonEBP [22]. Functional analysis of this protein, TonEBP/NFAT5, has clarified that it is induced upon hyperosmotic stimuli and is a target of integrin signaling [23]. Here we showed its potential to bind to the UCR of murine retroviruses and positively regulate their expression.

Engineering of the UCR Enhances the Reporter Gene Expression in Hepatocellular Carcinoma Cell Lines *in Vitro*

We have identified two regions important for retroviral expression. The first one contains a target of NFAT5 and the second one is known to be a target of Sp1 [11]. Since these transcription factors are expressed ubiquitously in a variety of tissues, but not restricted to hepatocytes [24,25], we made an attempt to examine whether the replacement of these target sequences increases specificity without lowering potency of retroviral expression in hepatocytes.

Hepatitis B virus (HBV) predominantly infects hepatocytes and the HBV genes are expressed specifically in liver, controlled by the combined action of the promoters and enhancers. The transcription of the viral mRNAs is regulated by two HBV enhancers, Enhancer I (EnI) and EnII, and the latter shows strong hepatocyte specificity [26,27]. We replaced two regions within the SFFVp U3 with the sequences from HBV EnII (specified as "a" or "b" in Fig. 5A), which determine the strong hepatocyte specificity and contain the targets of C/EBP, HNF4, HNF3, and HNF1. As shown in Fig. 5B, LTRs of pSF/Hep3-luc and pSF/Hep5-luc especially showed significantly higher promoter activity than the SFFVp LTR in PLC/PRF/5 cells ($P < 0.005$, Fig. 5B).

We generated two retroviral vectors, SF-Hep3/CAT and SF-Hep5/CAT, which contained the LTRs from pSF/Hep3-luc and pSF/Hep5-luc, respectively (Fig. 6A). First, we examined the efficiencies of the viral production of these novel vectors. Using Phoenix-eco packaging cells, titers of SF-Hep3/CAT and SF-Hep5/CAT were 5.7×10^5 and 6.0×10^5 G418-resistant colony-forming units per milliliter on NIH/3T3 cells (CFU-G418/ml), respectively, and were comparable with that of SF/CATwt (6.7×10^5 CFU-G418/ml). Next, we examined the activities of these engineered enhancers upon stable integration into the genome in

doi:10.1016/j.ymthe.2003.08.005

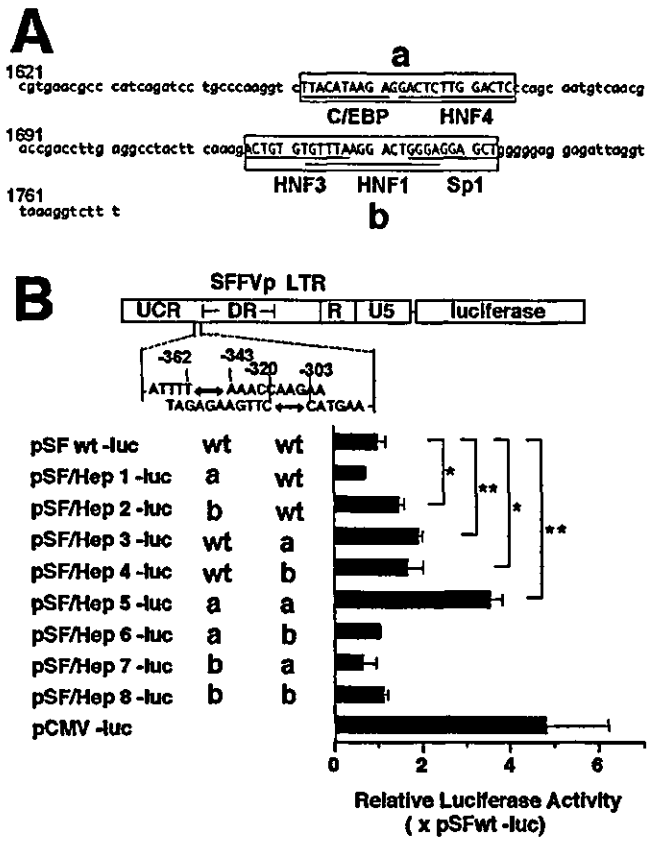

FIG. 5. Transient reporter gene assays of plasmids containing engineered LTRs. These plasmids were transfected into PLC/PRF/5 cells. (A) Sequence of the HBV EnII region. Boxed regions a and b were used for engineering the SFFVp LTR. Underlined regions represent the motifs for C/EBP, HNF4, HNF3, HNF1, and Sp1. (B) PLC/PRF/5 cells were transfected with luciferase reporter plasmids containing engineered LTRs. wt, original sequence of the SFFVp UCR; a, b, replaced by the sequence indicated as boxed region a or b from HBV EnII, respectively. Each column and bar represents the mean value and standard deviation of three assays, respectively. Significant difference from the value mediated by pSFwt-luc is indicated (*$P < 0.05$ and **$P < 0.005$).

cultured cells using Phoenix-ampho or -eco packaging cells. After the infection by these vectors at a multiplicity of infection lower than 0.1, we selected cells in the presence of G418 and measured expression of CAT protein. Although the average copy numbers of the proviral DNAs were not significantly different (data not shown), SF-Hep5/CAT provided a higher CAT value than SF/CATwt in human hepatocellular carcinoma cells PLC/PRF/5, HLE [33], and HuH-7 [34]. SF-Hep3/CAT provided a higher CAT value than SF/CATwt in PLC/PRF/5 and HLE cells (Fig. 6A). On the other hand, CAT values were not increased in fibroblastic cells (NIH/3T3 and HEK293) or lymphoid cells (Jurkat). In a hematopoietic precursor cell line, K562, the values were lower than those obtained with SF/CATwt. These results showed that transgene expression was enhanced by the engineered LTRs only in hepatocellular carcinoma cells.

The Novel Vectors SF-Hep3 and SF-Hep5 Efficiently Express a Transgene in Murine Hepatocytes *in Vivo*

To test whether the engineered LTRs provide a high transgene expression *in vivo*, we infused mice with SF/CATwt, SF-Hep3/CAT, SF-Hep5/CAT, or a MoMLV-based vector, MO3/CAT [19] (Fig. 6B), after partial hepatectomy. First, transgene expression was compared among these vectors 4 days after infusion. LTRs of SF/CATwt, SF-Hep3/CAT, and SF-Hep5/CAT were from SFFVp, pSF/Hep3-luc, and pSF/Hep5-luc, respectively. Expression of CAT by SF/CATwt, SF-Hep3/CAT, or SF-Hep5/CAT was about 2.5-, 4-, or 9-fold higher, respectively, than that by the MoMLV-based vector, MO3/CAT, and SF-Hep5/CAT provided about 3.5-fold higher expression than SF/CATwt (Fig. 6C). Since a partial hepatectomy induces liver cell replication, we additionally compared transgene expression among these vectors after 1 month of infusion to evaluate the expression in quiescent hepatocytes. Expression of CAT by SF/CATwt, SF-Hep3/CAT, or SF-Hep5/CAT was about 1.6-, 4.5-, or 5-fold higher, respectively, than that by MO3/CAT, and both SF-Hep3/CAT and SF-Hep5/CAT provided about 3-fold higher expression than SF/CATwt (Fig. 6D).

These results indicated strongly improved expression of a transgene by engineered LTRs in hepatocytes *in vivo*. Thus, we developed novel vectors designated SF-Hep3 and SF-Hep5 (SFFVp-based vector for hepatocytes), which will provide high transgene expression in hepatocytes *in vivo*.

To increase the transgene expression in hepatocytes *in vivo*, we have compared the promoter activities of murine retroviruses [19] and engineered the LTR from SFFVp in this study. An alternative approach to increasing the expression is to use hepatocyte-specific internal promoters. Although both positive and negative influences can be transmitted between the LTR and such an internal promoter [28], it has been proven that the use of the α1-antitrypsin promoter or the ApoE enhancer–α1-antitrypsin promoter increased transgene expression in hepatocytes *in vivo* [29,30]. Intensive effort has also been put into the development of viral vectors based on adeno-associated virus [31] and lentiviruses [32]. Together with the development of these vectors, the novel vectors designated SF-Hep3 and SF-Hep5 will provide a useful tool in the field of experimental hepatology, as well as important mechanistic information for the development of vectors for liver-targeted gene therapy.

Materials and Methods

Cell lines. The human hepatocellular carcinoma cell lines PLC/PRF/5 [20], HLE [33], and HuH-7 [34]; fibroblastic cell lines HEK293 and HEK293T; and hematopoietic cell lines K562 and Jurkat were maintained in DMEM supplemented with 10% fetal calf serum. A murine fibroblastic cell line, NIH/3T3, was maintained in DMEM with 10% calf serum. Amphotropic and ecotropic retrovirus packaging cell lines Phoenix-ampho and Phoenix-eco (kindly provided by Dr. G. P. Nolan of Stanford University Medical

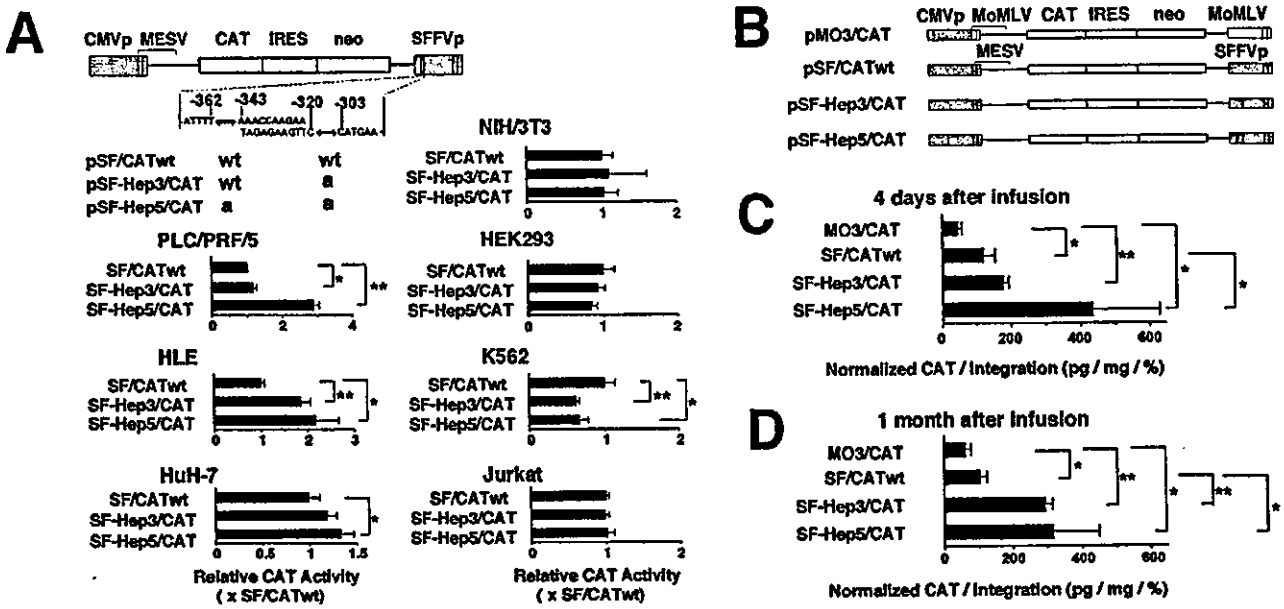

FIG. 6. Comparison of CAT gene expression among retroviral vectors *in vitro* and *in vivo*. Each column and bar represents the mean value and standard deviation of three assays, respectively. Significant difference (*$P < 0.05$ and **$P < 0.01$) from the value by SF/CATwt or MO3/CAT is indicated. (A) Retroviral vector plasmids were transiently transfected into Phoenix-ampho cells and the supernatants were used to transduce cell lines *in vitro*. wt, original sequence of the SFFVp UCR; a, b, replaced by the sequence indicated as boxed a or b (Fig. 5A) from HBV Enll, respectively. (B) Retroviral vector plasmids carrying a CAT gene are schematically shown. A MoMLV-based retroviral vector plasmid, pMO3/CAT, contains the LTR and the leader sequences from MoMLV [19]. FMEV-type retroviral vector plasmids, pSF/CATwt, pSF-Hep3/CAT, and pSF-Hep5/CAT, contain the wild-type or engineered LTRs of the SFFVp and the leader sequences from mouse embryonic stem cell virus (MESV) [16]. These plasmids were transiently transfected into Phoenix-eco cells and the supernatants were used to transduce hepatocytes *in vivo*. (C) The liver was removed 4 days after infusion. The concentration of CAT protein was normalized to the concentration of total proteins (pg/mg), further normalized to the proportion of integrated proviral DNA (%), and represented as "normalized CAT/integration (pg/mg/%)." Integration efficiencies of proviral DNAs into the liver ranged from 0.07 to 0.39% in this experiment. MO3/CAT, $n = 3$; SF/CATwt, $n = 3$; SF-Hep3/CAT, $n = 3$; SF-Hep5/CAT, $n = 3$. (D) The liver was removed 1 month after infusion. Integration efficiencies of proviral DNAs into the liver ranged from 0.10 to 0.49% in this experiment. MO3/CAT, $n = 4$; SF/CATwt, $n = 4$; SF-Hep3/CAT, $n = 3$; SF-Hep5/CAT, $n = 4$.

Center, Stanford, CA) [35], respectively, were cultured in DMEM with 10% fetal calf serum.

Construction of reporter gene plasmids. A series of luciferase reporter gene vectors, schematically shown in Fig. 1A, was constructed as follows. The U3 region of SFFVp (corresponding to the sequences from 4 to 418 bp upstream of the cap site; position −4 to −418) was amplified by polymerase chain reaction and was ligated into the *Eco*RV site of pBlueScript SK (pBS; Stratagene, La Jolla, CA) by the TA cloning technique. A *Bam*HI–*Hin*dIII fragment was excised and ligated into *Bgl*II–*Hin*dIII sites of the promoterless firefly luciferase reporter gene vector pGL3-Basic (Promega Japan, Tokyo), to obtain pSF418luc. Using the same strategy, pSF371luc, pSF352luc, pSF320luc, pSF289luc, pSF272luc, pSF238luc, pSF228luc, pSF178luc, and pSF118luc were constructed, which contain the U3 sequences from position −4 to −371, −352, −320, −289, −272, −238, −228, −178, and −118, respectively. A series of luciferase reporter gene vectors, schematically shown in Fig. 1B, was constructed as follows. A fragment of the SFFVp U3 (position −320 to −371) was amplified, ligated into pBS, excised as an *Xba*I–*Xho*I fragment, and ligated into *Nhe*I–*Xho*I sites of pSF178luc to obtain pSF371-320/178luc. Using the same strategy, pSF371-311/178luc, pSF371-303/178luc, pSF371-270/178luc, pSF371-253/178luc, and pSF371-208/178luc were constructed, which contain the sequences from position −311, −303, −270, −253, or −208 to −371, respectively. A series of reporter gene plasmids, schematically shown in Fig. 1C, was constructed as follows. A *Bgl*II–*Hin*dIII fragment of the thymidine kinase promoter of herpes simplex virus from pRL-TK (Promega Japan) was ligated into *Bgl*II–*Hin*dIII sites of pGL3-Basic to obtain a plasmid, pTKluc. A fragment containing the SFFVp U3 (position from −303 to −362) was amplified, ligated into pBS (pBS362-303), excised as a *Xba*I–*Xho*I fragment, and ligated into *Nhe*I–*Xho*I sites of pTKluc to obtain p362-303TKluc. Using the same strategy, p371-311TKluc, p371-303TKluc, and p352-303TKluc were obtained, which contain the sequences from position −371 to −311, from −371 to −303, and from −352 to −303, respectively. Plasmid p303-371TKluc was obtained from a fragment containing the sequence from −303 to −371 in the direction opposite to p371-303TKluc. A series of reporter gene plasmids, schematically shown in Fig. 1D, was constructed as follows. Plasmid DNA of pBS362-303 was amplified by PCR, phosphorylated, self-ligated (pBS362-343/320-303), excised as an *Xba*I–*Xho*I fragment, and ligated into *Nhe*I–*Xho*I sites of pTKluc to obtain p362-343/320-303TKluc. Using the same strategy, p371-352/320-303TKluc and p371-343/320-303TKluc were obtained, in which the sequence from position −351 to −321 or from −342 to −321, respectively, was deleted. The sequence from position −352 to −371 or from −303 to −320 was further deleted from p371-352/320-303TKluc or p362-343/320-303TKluc to obtain p320-303TKluc or p362-343TKluc, respectively. All these plasmids were sequenced before the experiments. A reporter gene plasmid containing tandem repeats of the *cis*-regulatory element is schematically shown in Fig. 4D. The following pair of oligonucleotides was annealed, ligated into the *Eco*RV site of pBS, excised as an *Xba*I–*Xho*I fragment, and ligated into *Nhe*I–*Xho*I sites of pTKluc to obtain p362-343×4TKluc, which contains four tandem repeats of the sequence from position −343 to −362: 5′-GCAAGGCATGGAAAAATACCGCAAGGCATGGAAAAATACCGCAAGGCATGGAAAAATACCGCAAGGCATGGAAAAATACC-3′ and 5′-GGTATTTTTCCATGCCTTGCGGTATTTTTCCATGCCTTGCGGTATTTTTCCATGCCTTGCGGTATTTTTCCATGCCTTGC-3′.

doi:10.1016/j.ymthe.2003.08.005

Construction of reporter gene plasmids for mutation analysis of the cis-regulatory elements. A series of reporter gene plasmids, schematically shown in Fig. 3A, was constructed as follows. The three to four base pair substitution mutations (A → G, T → C, C → T, G → A) were sequentially introduced from 5′ to 3′ into pBS362-343/320-303 using the Quick Change mutagenesis kit. After sequencing, an *XbaI–XhoI* fragment was excised and ligated into *NheI–XhoI* sites of pTKluc to obtain pMut/1 to pMut/10.

Construction of a plasmid for the expression of NFAT5. A human NFAT5 cDNA was amplified by reverse transcriptase-polymerase chain reaction from human liver cDNA and ligated into *BamHI–XhoI* sites of a mammalian expression vector, pCMV-Tag2 (Stratagene), to obtain pCMV/flag-NFAT5.

Construction of retroviral vector plasmids. The U3 region of the 5′ LTR of pSF1N was replaced by a human cytomegalovirus promoter to obtain pSF1N/CMV. A plasmid DNA of pBS/LTR was amplified, self-ligated, excised, and ligated into *BamHI–XhoI* sites of pSF/CMV to generate pSF1N/Δ362-343, pSF1N/Δ320-303, or pSF1N/Δ362-343/320-303. A *NotI–NotI* fragment containing a CAT gene at the 5′ position and internal ribosomal entry site from poliovirus was ligated into a *NotI* site of pSF/CMV, pSF1N/Δ362-343, pSF1N/Δ320-303, or pSF1N/Δ362-343/320-303 to obtain pSF/CATwt, pSF/CATΔ362-343, pSF/CATΔ320-303, or pSF/CATΔ362-343/320-303, respectively. Construction of pMO3/CAT was described elsewhere [19].

Construction of plasmids containing engineered LTRs. A series of reporter gene plasmids or retroviral vector plasmids containing the engineered LTRs is schematically shown in Fig. 5B or 6A, respectively. A *BamHI–XhoI* fragment containing the 3′ LTR was ligated into pBS and plasmid DNA was amplified by PCR and ligated with annealed oligonucleotides (a) 5′-TTACATAAGAGGACTCTTGGACTCA-3′ and 5′-TGAGTCCAAGAGTCCTCTTATGTAA-3′ or (b) 5′-ACTGTGTGTTTAAGGACTGGGAGGAGCTA-3′ and 5′-TAGCTCCTCCCAGTCCTTAAACACACAGT-3′. *SpeI–XhoI* or *BamHI–XhoI* fragments containing engineered LTRs were ligated into *NheI–XhoI* sites of pGL3-basic or *BamHI–XhoI* sites of pSF/CATwt to obtain pSF/Hep1-luc to pSF/Hep8-luc or pSF-Hep3/CAT and pSF-Hep5/CAT, respectively.

Transient transfection and reporter gene assays. For transient reporter assays, 10 μg of firefly luciferase reporter gene vector DNAs was cotransfected with pRL-CMV or pRL-TK (a *Renilla* luciferase vector; Promega Japan) DNA by calcium phosphate coprecipitation method as described [18]. Transfected cells were harvested after 48 h of incubation and luciferase activities were measured according to the Promega protocols and applications guide by using the Dual-Luciferase Reporter Assay System (Promega Japan) with the Turner Designs luminometer Model TD-20/20 (Promega Japan). The firefly luciferase activity of each lysate was normalized to the activity of *Renilla* luciferase and was represented as activity relative to that of pSF418luc, pTKluc, or p362-343/320-303TKluc. In some experiments, plasmids for the expression of transcription factors were additionally transfected into cells.

Production of retroviral vectors. Phoenix-ampho or Phoenix-eco cells were transfected with retroviral vector plasmids. After 2–5 days of culture, supernatant containing viral vectors was used in this study. Viral vectors were termed SF/CATwt, SF/CATΔ362-343, SF/CATΔ320-303, SF/CATΔ362-343/320-303, MO3/CAT, SF-Hep3/CAT, or SF-Hep5/CAT to distinguish them from the corresponding plasmids.

Retroviral transduction and measurement of CAT protein and copy numbers of integrated proviral DNAs. Cells were infected with SF/CATwt, SF/CATΔ362-343, SF/CATΔ320-303, SF/CATΔ362-343/320-303, SF-Hep3/CAT, or SF-Hep5/CAT and were selected in the presence of G418 for 2 weeks. After selection, cells consisting of more than 100 different clones were lysed and the concentration of CAT protein of each lysate was measured by using a CAT enzyme-linked immunosorbent assay kit (Boehringer Mannheim GmbH, Mannheim, Germany). The concentration of CAT protein in each lysate was normalized to the concentration of total proteins (pg/mg) and was represented as CAT activity relative to that of SF/CATwt. To confirm that the copy numbers of integrated proviral DNAs in pooled cells were not significantly different among the vectors, TaqMan real-time PCR was performed after genomic DNAs were isolated from the samples. Genomic DNAs from clones containing one or two proviral integrations were used as standards. The estimated numbers were further normalized to β-actin using the following primers and probes: CAT primers, 5′-GTTTTCATCGCTCTGGAGTGAA-3′, 5′-CACGCCACATCTTGCGAATATA-3′; CAT probe, 5′-CCACGACGATTTCCGGCAGTTTCTAC-3′; mouse β-actin primers, 5′-AAGAGCTATGAACTGCCTGACG-3′ and 5′-CAAGAAGGAAGGCTGGAAAAGA-3′; mouse β-actin probe, 5′-CCCCTCCCCAGTAAAGGCTTCTGTAGAGAG-3′; human β-actin primers; and a probe, TaqMan β-actin detection reagents kit (PE Applied Biosystems Japan, Tokyo).

In vivo experiments were performed as described previously [19]. In brief, virus particles were produced using Phoenix-eco packaging cells and were concentrated [36]. Forty-eight hours after partial hepatectomy, C57/BL6 mice were infused via the tail vein with viruses representing infusion of $3–5 \times 10^6$ G418-resistant colony-forming units on NIH/3T3 cells. Four days or 1 month after infusion, the liver was removed and the concentration of CAT protein in each lysate was normalized to the concentration of total proteins (pg/mg). Genomic DNAs from the samples were isolated and the proportions of the genomic integration of proviral DNAs were estimated by the TaqMan real-time PCR method. A genomic DNA from a NIH/3T3 clone containing a single integrated copy and that from an uninfected clone were mixed at a ratio ranging from 1:1000 to 1:10 and were used as standards. The estimated proportion was normalized to β-actin to determine the integration efficiencies (%). Normalized concentration of CAT protein of each sample (pg/mg) was further normalized to the integration efficiency (%) and was represented as normalized CAT/integration (pg/mg/%) in Figs. 6C and 6D.

Western blotting and gel mobility shift assays. After the transfection of pCMV/flag-NFAT5 into HEK293T cells, cell lysate was analyzed by Western blot using an antibody to flag (M2; Sigma, St. Louis, MO). Preparations of nuclear extracts and gel mobility shift assays were performed as previously described [11]. The following set of oligonucleotides was annealed and used for this study: GGCAAGGCATGGAAAAATAC and GGTATTTTTCCATGCCTTGC. Supershift assays using an antibody to flag (M2; Sigma) were performed by incubating antibodies with nuclear extract for 1 h at 4°C.

Acknowledgments

This work was partly supported by Grants-in-Aid from the Ministry of Education, Science, Sports, and Culture of Japan.

RECEIVED FOR PUBLICATION APRIL 29, 2003; ACCEPTED AUGUST 14, 2003.

References

1. Mulligan, R. C. (1993). The basic science of gene therapy. *Science* 260: 926–932.
2. Robbin, P. D., and Ghivizzni, S. C. (1998). Viral vectors for gene therapy. *Pharmacol. Ther.* 80: 35–47.
3. Kay, M. A., *et al.* (1993). *In vivo* gene therapy of hemophilia B: sustained partial correction in factor IX-deficient dogs. *Science* 262: 117–119.
4. Kay, M. A. (1998). Hepatic gene therapy for haemophilia B. *Haemophilia* 4: 389–392.
5. Golemis, E. A., Speck, N. A., and Hopkins, N. (1990). Alignment of U3 region sequences of mammalian type C viruses: identification of highly conserved motifs and implications for enhancer design. *J. Virol.* 64: 534–542.
6. Wang, S., *et al.* (1993). Cloning and characterization of subunits of the T-cell receptor and murine leukemia virus enhancer core-binding factor. *Mol. Cell. Biol.* 13: 3324–3339.
7. Nielsen, A. L., Norby, P. L., Pedersen, F. S., and Jorgensen, P. (1996). Various modes of basic helix–loop–helix protein-mediated regulation of murine leukemia virus transcription in lymphoid cell lines. *J. Virol.* 70: 5893–5901.
8. Barat, C., and Rassart, E. (1998). Members of the GATA family of transcription factors bind to the U3 region of Cas-Br-E and graffi retroviruses and transactivate their expression. *J. Virol.* 72: 5579–5588.
9. Granger, S. W., and Fan, H. (1998). *In vivo* footprinting of the enhancer sequences in the upstream long terminal repeat of Moloney murine leukemia virus: differential binding of nuclear factors in different cell types. *J. Virol.* 72: 8961–8970.
10. Zaiman, A. L., Nieves, A., and Lenz, J. (1998). CBF, Myb, and Ets binding sites are

important for activity of the core I element of the murine retrovirus SL3-3 in T lymphocytes. *J. Virol.* 72: 3129–3137.
11. Baum, C., *et al.* (1997). The potent enhancer activity of the polycythemic strain of spleen focus-forming virus in hematopoietic cells is governed by a binding site for Sp1 in the upstream control region and by a unique enhancer core motif, creating an exclusive target for PEBP/CBF. *J. Virol.* 71: 6323–6331.
12. Tsukiyama, T., Ueda, H., Hirose, S., and Niwa, O. (1992). Embryonal long terminal repeat-binding protein is a murine homolog of FTZ-F1, a member of the steroid receptor superfamily. *Mol. Cell. Biol.* 12: 1286–1291.
13. Flanagan, J. R., Krieg, A. M., Max, E. E., and Khan, A. S. (1989). Negative control region at the 5′ end of murine leukemia virus long terminal repeats. *Mol. Cell. Biol.* 9: 739–746.
14. Wahlers, A., *et al.* (2002). Upstream conserved sequences of mouse leukemia viruses are important for high transgene expression in lymphoid and hematopoietic cells. *Mol. Ther.* 6: 313–320.
15. Ostertag, W., *et al.* (1987). Transforming genes and target cells of murine spleen focus-forming viruses. *Adv. Cancer Res.* 48: 193–355.
16. Baum, C., Hegewisch-becker, S., Eckert, H.-G., Stocking, C., and Ostertag, W. (1995). Novel retroviral vectors for efficient expression of the multidrug resistance (mdr-1) gene in early hematopoietic cells. *J. Virol.* 69: 7541–7547.
17. Tsuji, T., *et al.* (2000). Retroviral vector-mediated gene expression in human $CD34^+CD38^-$ cells expanded *in vitro*: cis elements of FMEV are superior to those of Mo-MuLV. *Hum. Gene Ther.* 11: 271–284.
18. Danno, S., *et al.* (1999). Efficient gene transfer by hybrid retroviral vectors to murine spermatogenic cells. *Hum. Gene Ther.* 10: 1819–1831.
19. Ohnishi, N., *et al.* (2002). High expression of transgenes mediated by hybrid retroviral vectors in hepatocytes: comparison of promoters from murine retroviruses *in vitro* and *in vivo*. *Gene Ther.* 9: 303–306.
20. Knowles, B. B., Howe, C. C., and Aden, D. P. (1980). Human hepatocellular carcinoma cell lines secrete the major plasma proteins and hepatitis B surface antigen. *Science* 209: 497–499.
21. Chen, L., Glover, J. N., Hogan, P. G., Rao, A., and Harrison, S. C. (1998). Structure of the DNA-binding domains from NFAT, Fos and Jun bound specifically to DNA. *Nature* 392: 42–48.
22. Miyakawa, H., Woo, S. K., Dahl, S. C., Handler, J. S., and Kwon, H. M. (1999). Tonicity-responsive enhancer binding protein, a rel-like protein that stimulates transcription in response to hypertonicity. *Proc. Natl. Acad. Sci. USA* 96: 2538–2542.
23. Jauliac, S., *et al.* (2002). The role of NFAT transcription factors in integrin-mediated carcinoma invasion. *Nat. Cell Biol.* 4: 540–544.
24. Lopez-Rodriguez, C., Aramburu, J., Rakeman, A. S., and Rao, A. (1999). NFAT5, a constitutively nuclear NFAT protein that does not cooperate with Fos and Jun. *Proc. Natl. Acad. Sci. USA* 96: 7214–7219.
25. Black, A. R., Black, J. D., and Azizkhan-Clifford, J. (2001). Sp1 and kruppel-like factor family of transcription factors in cell growth regulation and cancer. *J. Cell. Physiol.* 188: 143–160.
26. Wang, Y., *et al.* (1990). A new enhancer element, ENII, identified in the X gene of hepatitis B virus. *J. Virol.* 64: 3977–3981.
27. Su, H., and Yee, J. K. (1992). Regulation of hepatitis B virus gene expression by its two enhancers. *Proc. Natl. Acad. Sci. USA* 89: 2708–2712.
28. Wu, X., Holschen, J., Kennedy, S. C., and Ponder, K. P. (1996). Retroviral vector sequences may interact with some internal promoters and influence expression. *Hum. Gene Ther.* 7: 159–171.
29. Hafenrichter, D. G., Wu, X., Rettinger, S. D., Kennedy, S. C., Flye, M. W., and Ponder, K. P. (1994). Quantitative evaluation of liver-specific promoters from retroviral vectors after *in vivo* transduction of hepatocytes. *Blood* 84: 3394–3404.
30. Okuyama, T., *et al.* (1996). Liver-directed gene therapy: a retroviral vector with a complete LTR and the ApoE enhancer-alpha 1-antitrypsin promoter dramatically increases expression of human alpha 1-antitrypsin *in vivo*. *Hum. Gene Ther.* 7: 637–645.
31. Snyder, R. O., *et al.* (1997). Persistent and therapeutic concentrations of human factor IX in mice after hepatic gene transfer of recombinant AAV vectors. *Nat. Genet.* 16: 270–276.
32. Park, F., Ohashi, K., Chiu, W., Naldini, L., and Kay, M. A. (2000). Efficient lentiviral transduction of liver requires cell cycling *in vivo*. *Nat. Genet.* 24: 49–52.
33. Doi, I., Mamba, M., and Sato, J. (1975). Establishment and some characteristics of human hepatoma cell lines. *Jpn. J. Cancer Res.* 66: 385–392.
34. Nakabayashi, H., Taketa, K., Miyano, K., Yamane, T., and Sato, J. (1982). Growth of human hepatoma cells lines with differentiated functions in chemically defined medium. *Cancer Res.* 42: 3858–3863.
35. Kitamura, T., Onishi, M., Kinoshita, S., Shibuya, A., Miyajima, A., and Nolan, G. P. (1995). Efficient screening of retroviral cDNA expression libraries. *Proc. Natl. Acad. Sci. USA* 92: 9146–9150.
36. Yang, J., Friedman, M. S., Bian, H., Crofford, L. J., Roessler, B., and McDonagh, K. T. (2002). Highly efficient genetic transduction of primary human synoviocytes with concentrated retroviral supernatant. *Arthritis Res.* 4: 215–219.

tapraid2/zg0-gast/zg0-gast/zg000205/zg01756d05z | xppws | S=1 | 1/4/05 | Art: 51756 | DTD5.0

GASTROENTEROLOGY 2005;128:449–462

La Protein Is a Potent Regulator of Replication of Hepatitis C Virus in Patients With Chronic Hepatitis C Through Internal Ribosomal Entry Site–Directed Translation

MASAO HONDA, TAKEO SHIMAZAKI, and SHUICHI KANEKO
Department of Gastroenterology, Kanazawa University Graduate School of Medicine, Kanazawa, Japan

Background & Aims: Translation of hepatitis C virus is an essential step of viral replication and is mediated by an internal ribosome entry site. We previously reported that the hepatitis C virus internal ribosome entry site is most active during the synthetic (S) or mitotic (M) phases and lowest during quiescent (G_0) phase. Here, we investigated host factors responsible for the regulation of the hepatitis C virus internal ribosome entry site. *Methods:* We synchronized the cell-cycle progression and evaluated gene-expression dynamics of host factors and kinetics of hepatitis C virus internal ribosome entry site activity in cells at various points during the cell cycle by using a complementary DNA microarray. We also validated the significance of identified host factors on hepatitis C virus replication in vivo. *Results:* Hepatitis C virus internal ribosome entry site activity correlated with a gene cluster induced in the S and G_2/M phases. It is interesting to note that most initiation factors known to bind or interact with the hepatitis C virus internal ribosome entry site [poly(rC)-binding protein 2, polypyrimidine tract binding protein, eukaryotic initiation factor 3, eukaryotic initiation factor 2γ, eukaryotic initiation factor 2β, La protein, and RNLPL] were induced during the S and G_2/M phases. Expression of La protein, polypyrimidine tract binding protein, and eukaryotic initiation factor 3 (p116, 170) were predominantly repressed in G_0 phase and induced in S and G_2/M phases. Suppression or overexpression of La protein and polypyrimidine tract binding protein in RCF-26 significantly changed hepatitis C virus internal ribosome entry site activity. In the livers of patients with chronic hepatitis C, expression of La protein was significantly increased and correlated with the amount of hepatitis C virus RNA. *Conclusions:* Hepatitis C virus uses host factors induced during cell division but not during quiescence for replication. Of these, La protein is a potent regulator and enhances hepatitis C virus replication in regenerating hepatocytes in patients with chronic hepatitis C.

Hepatitis C virus (HCV), a positive-strand enveloped RNA virus, belongs to the genus *Hepacivirus* of the family Flaviviridae.[1] The human liver infected with HCV develops chronic hepatitis, cirrhosis, and, in some instances, hepatocellular carcinoma.[1,2] Although a combination of ribavirin and interferon has become a popular means of treating infected patients, the results are often unsatisfactory, especially in patients with a high viral load.[3–6] Identification of host factors that regulate HCV replication in infected patients could be helpful in the development of a novel antiviral treatment strategy.

Translation of the polyproteins of the HCV RNA genome is an essential step in viral replication and is supposed to be a fruitful target of new antiviral treatment strategies, such as antisense oligonucleotide (oligo) or small interference RNA. Translation of HCV is initiated by a highly structured RNA segment, the internal ribosome entry site (IRES), that occupies most of the 5′-nontranslated (5′-NTR) RNA.[7–15] The translation machinery of HCV is simple and, because it is a prokaryote, requires only the ribosomal 40S subunit, the eukaryotic initiation factor (eIF)2/guanosine triphosphate/Met-transfer RNA complex, and eIF3 to initiate translation.[7] In contrast, cap-dependent translation is more complex and requires additional canonical initiation factors, such as eIF4E, eIF4G, eIF4A, and eIF4B.[7] Many other noncanonical translation initiation factors, such as La protein,[16,17] polypyrimidine tract binding protein (PTB),[18] heterogeneous nuclear ribonucleoprotein L (RNPL),[19] poly(rC)-binding protein (PCBP)-2,[20] and ribosomal protein S9,[7] interact with HCV IRES and might regulate HCV translation. Thus, the machineries of cap-dependent and HCV IRES–directed translation

Abbreviations used in this paper: CMV, cytomegalovirus; eIF, eukaryotic initiation factor; FBS, fetal bovine serum; FL, firefly luciferase; IRES, internal ribosomal entry site; nt, nucleotide; 5′-NTR, 5′ nontranslated region; oligo, oligonucleotide; PABPC, poly(A)-binding protein, cytoplasmic; PCBP, poly(rC)-binding protein; PTB, polypyrimidine tract binding protein; RL, renilla luciferase; RNPL, heterogeneous nuclear ribonucleoprotein L; RTD, real-time detection; RT-PCR, reverse-transcription polymerase chain reaction; SOM, self-organizing map.

0016-5085/05/$30.00
doi:10.1053/j.gastro.2004.11.064

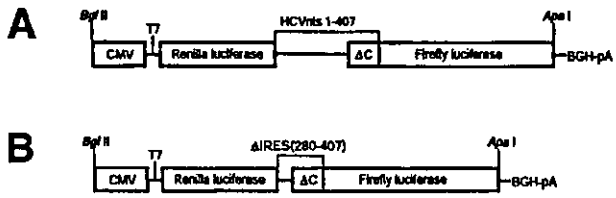

Figure 1. Organization of the transcriptional unit of plasmid pRL-HL and pRL-(ΔIRES)-HL. (*A*) Plasmid pRL-HL[22] contains a dicistronic CMV transcriptional cassette in which upstream renilla and downstream firefly luciferase genes are separated by the complete 5′-NTR and 66-nt core sequence of HCV (nts 1–407; strain 1b) placed in the intercistronic space. (*B*) Plasmid pRL-(ΔIRES)-HL was the control plasmid of pRL-HL in which the functional HCV IRES element (nts 1–279) was deleted. CMV, cytomegalovirus promoter; T7, Bacteriophage T7 RNA polymerase promoter; BGH-pA, bovine growth hormone polyadenylation signal.

can be differentiated in terms of requirements for canonical and noncanonical initiation factors.[21]

We previously found that HCV IRES activity varies during the cell cycle and is greatest during the synthetic (S) or mitotic (M) phases and lowest during the quiescent (G_0) phase.[22] These findings suggest that HCV translation is regulated by cellular proteins that vary in abundance during the cell cycle and that viral replication is enhanced by factors that stimulate the regeneration of hepatocytes in patients with chronic hepatitis C. This finding implies that inflammation and the resulting increased turnover in hepatocytes may increase the number of actively dividing hepatocytes, resulting in increased IRES activity and enhanced HCV replication.

This study profiles the expression of cellular proteins during cell-cycle progression and identifies factors responsible for cell cycle–dependent HCV IRES–directed translation. We evaluated whether those factors are in fact related to HCV replication in the livers of patients with chronic hepatitis C.

Materials and Methods

●●●Plasmids

Plasmid pRL-HL contains a dicistronic cytomegalovirus (CMV) transcriptional cassette in which an upstream renilla luciferase (RL) gene and a downstream firefly luciferase (FL) gene are separated by the complete 5′-NTR and 66-nucleotide (nt) core sequence of HCV (nts 1–407 of a genotype 1b strain) placed within the intercistronic space[22] (Figure 1*A*). Plasmid pRL-(ΔIRES)-HL was the control plasmid of pRL-HL in which the functional HCV IRES element (nts 1–279) had been deleted (Figure 1*B*). This plasmid was constructed by subcloning the 1.82-kilobase *StuI/ApaI* fragment of pRL-HL (containing the deleted HCV IRES element [nts 280–341 of the HCV-1b 5′-NTR sequence and 66 nts of the core sequence] fused directly to FL) into the multiple cloning site of pBluescript IISK (Stratagene). A 1.82-kilobase *NotI/ApaI* fragment was subsequently excised from this plasmid and cloned into the *NotI/ApaI* site of pRL-HL.

The La expression vector pCMV-La was constructed as previously described.[23] The PTB expression vector pRC/CMV-PTB, the RNPL expression vector pcDNA3-myc-hnRNPL, and the PCBP-1 and PCBP-2 expression vectors pcDNA3-myc-haCP1 and pcDNA3-myc-haCP2 were provided by Dr. Stanley M. Lemon,[24] Dr. Gideon Dreyfuss,[25] and Dr. Stephen A. Liebhaber,[26] respectively. Dr. John W. B. Hershey provided the eIF2γ full-length clone in pSP72.[27] We constructed the eIF2γ expression vector pCMV-eIF2-γ by excising the *Eco*RI and *Eco*RI fragment of full-length coding sequences and cloning into *Eco*RI of pCR 3.1 (Invitrogen, San Diego, CA) under the control of the CMV promoter. Dr. Keith Johnson provided the eIF3 p170 full-length clone in PUC19.[28] We constructed the eIF3 p170 expression vector pCMV-eIF3 p170 by excising the *Kpn*I and *Sna*BI fragment of full-length coding sequences and cloning into *Kpn*I and *Eco*RV of pCR 3.1 under the control of the CMV promoter. The complementary DNA (cDNA) of ribosomal protein S9 was cloned by reverse-transcription polymerase chain reaction (RT-PCR) of total RNA isolated from Huh-7 cells by using sense (5′-ACGGTGGAAGCGGACG-CAACATGCCAGTGG-3′) and antisense (5′-GGGACAG-GTGGACTTAATCCTCCTCCTCGTCG-3′) primers. The resultant cDNA was cloned into the TOPO TA cloning vector (Invitrogen), and nt sequences were confirmed. The expression vector pCMV-S9 was constructed by excising and cloning *Hin*dIII and *Xho*I fragments from TOPO TA into the same sites of pCR 3.1.

Cell Lines

The RCF-26 was a stably transformed cell line from Huh-7 cells (human hepatocellular carcinoma cells) that constitutively express dicistronic RNA transcripts containing sequences encoding 2 reporter proteins, RL and FL, separated by a functional HCV IRES[22] (Figure 1*A*). The ΔRCF-9 was a stably transformed cell line from Huh-7 cells that constitutively expressed dicistronic RNA transcripts in which the functional HCV IRES element (nts 1–279) had been deleted (Figure 1*B*).

Overexpression of Canonical and Noncanonical Initiation Factors in RCF-26

The RCF-26 cells were cultured in Dulbecco's modified Eagle medium (Gibco BRL, Gaithersburg, MD) containing 10% fetal bovine serum (FBS), 1% penicillin/streptomycin, and 400 μg/mL of Geneticin (active compound). Cells cultured in a 5% CO_2 incubator at 37°C were transfected with 0.5–1.0 μg of plasmid DNA by using FuGENE 6 (Roche Molecular Biochemicals, Basel, Switzerland) according to the manufacturer's instructions. After 24–48 hours of transfection, the cells were harvested, and reporter genes were assayed.

Reporter Gene Assays

Cells cultured in 10- or 15-cm dishes in Dulbecco's modified Eagle medium containing 10% FBS were trypsinized.

taprald2/zg0-gast/zg0-gast/zg000205/zg01756d05z | xppws | S=1 | 1/4/05 | Art: 51756 | DTD5.0

A quarter of the cells were lysed in 1 mL of passive lysis buffer (25 mmol/L Tris-phosphate [pH 7.8], 2 mmol/L dithiothreitol, 2 mmol/L 1,2-diaminocyclohexane-N,N,N′,N′-tetraacetic acid, 10% glycerol, and 1% Triton X-100). RL and FL activities were measured in 20 μL of cell lysate by using the Dual-Luciferase Reporter Assay System (Promega, Madison, WI). Total RNA was isolated from the remainder and processed for analysis by cDNA microarray, Northern blotting, and real-time detection (RTD) PCR.

Antisense Oligodeoxynucleotide

We designed respective antisense phosphorothioate oligos that were complementary to the sequence from 5 nts upstream to 15 downstream of the predicted translational initiation site of the La protein, PTB, eIF3 p170, eIF2γ, RNPL, poly(A)-binding protein, cytoplasmic 1 (PABPC-1), PCBP-2, and ribosomal protein S9 gene. The nt sequences of antisense oligos were 5′-GCCATTACGGCTATCTTTAA-3′ for La protein, 5′-TCCATGGCACACAGAGCAGA-3′ for PTB, 5′-GGCATTTTCCGGCCTCTGAA-3′ for eIF3 p170, 5′-CCAGCTTCTCCGCCCGCCAT-3′ for eIF2γ, 5′-ACCATCGCTCCCGACCGCCT-3′ for RNPL, 5′-TTCATCTCGGCACGGCTGCC-3′ for PABPC-1, 5′-TCCATGTCGAGCAGTGTTCT-3′ for PCBP-2, and 5′-GGCATGTTGCGTCCGCTTCCGCC-3′ for ribosomal protein S9. Positive and negative controls consisted of an antisense oligo for the 5′ region of HCV (nt 330–350), 5′-GTGCTCATGGTGCACGGTCT-3′,[29] and the randomized oligo, 6961, 5′-TACGTTTCTATGTCGATGGG-3′,[29] respectively. Oligodeoxynucleotides (0.5–1.0 μmol/L) were added to the medium by using the FuGENETM6 transfection reagent (Boehringer Mannheim, Mannheim, Germany), and the cultures were incubated for 24 hours. Cells were harvested, and HCV IRES activity was evaluated by assaying the reporter genes. To validate repressed targeted gene expression, 1 μg of total RNA was amplified by RT-PCR with specific primers for La protein, PTB, eIF3 p170, and ribosomal protein S9. The internal control was the level of β-actin expression.

Synchronization of Cell Growth and Analysis of Cellular DNA Content

To examine the relationship between HCV IRES–directed translation and cell growth, RCF-26 cells and ΔRCF-9 cells were incubated in 15-cm dishes with low serum or at confluence for 24–48 hours. RCF-26 cells and ΔRCF-9 cells in 10-cm dishes were synchronized at the G_1/S phase border by starvation for 24 hours in medium containing 0.1% FBS, followed by a wash and an 18-hour incubation in medium containing 10% FBS and 2.5 μg/mL aphidicolin. Aphidicolin was removed from the synchronized cells by washing and adding fresh medium containing 1% FBS. The cells were harvested at 3-hour intervals over 48 hours to assess the cell-cycle phase and reporter enzyme activities. The cell-cycle phase distribution in each sample cell population was determined by measuring the DNA content of individual cells by flow cytometry.[22]

Complementary DNA Microarray Analysis

We profiled gene expression in cells at different phases of the cell cycle by cDNA microarray analysis. We reconstructed the gene set of cDNA microarray slides containing 1080 cDNA clones[30] by adding canonical and noncanonical initiation factors. The new microarray included La protein,[16] PTB,[18] eIF2β,[31] eIF2γ,[31] eIF3 p116, eIF3 p170,[32] RNPL,[19] ribosomal protein S9,[7] PCBP-2,[20] PABPC-1,[33] and cell division cycle 2–like 1 proteins (PITSLRE proteins)[34] that bind HCV or other viral IRES structures and might affect the IRES activity. Other canonical initiation factors, such as eIF1A, eIF2A, eIF4A, eIF4B, eIF4E, and eIF5,[7,21,35] were also included to analyze cap-dependent translation machinery.

Total RNA (50 μg) isolated from serum-starved or confluent cells (10% FBS and at 60%–70% cell density) was labeled with a fluorescent dye for the cDNA microarray.[30,36,37] To profile gene expression in cells during the cell cycle, total RNA was periodically extracted from synchronized cells at 3, 9, 15, 18, 24, 30, 36, and 42 hours released from aphidicolin block (G_1/S border). After 1 round of amplification, antisense RNA was labeled and hybridized with the cDNA microarray.[30,36,37] Images were acquired, and cDNA microarray slides were analyzed as previously described.[30,36,37] A 1-dimensional self-organizing map (SOM) was constructed to cluster genes with a similar expression profile throughout cell-cycle progression (cluster and tree view; http://rana.Stanford.EDU/software/).

Northern Blotting

We evaluated La protein, PTB, and albumin expression in cultured cells and in tissue samples by Northern blotting. Total RNA (20 μg) was separated on denaturing agarose/formaldehyde gels, transferred to a membrane, and hybridized with specific probes under standard conditions.

Western Blotting

RCF-26 cells seeded in a 10-cm dish were grown to subconfluency and washed twice with phosphate-buffered saline. Cells were lysed in radioimmunoprecipitation assay buffer. Cell lysates were collected by pelleting cell debris, and the concentration of protein was quantified by using a dye-binding assay (Bio-Rad, Hercules, CA). Eighty micrograms of cell lysate was electrophoresed in a sodium dodecyl sulfate/12.5% polyacrylamide gel and electrotransferred to a nitrocellulose membrane. After blocking with phosphate-buffered saline with 0.3% Tween-20 containing 5% skim milk for 1 hour, the membranes were reacted with appropriate antibodies. After washing with phosphate-buffered saline with 0.3% Tween-20, membranes were reacted with horseradish peroxidase–conjugated anti-mouse immunoglobulin G or anti-rabbit immunoglobulin G antibodies diluted 1:3000. Membranes were washed again and then visualized with an enhanced chemiluminescence kit (Amersham Pharmacia Biotech, Uppsala, Sweden).

taprald2/zg0-gast/zg0-gast/zg000205/zg01756d05z | xppws | S=1 | 1/4/05 | Art: 51756 | DTD5.0

Real-Time Detection Polymerase Chain Reaction

The PCR reaction mixture was prepared by using TaqMan Universal Master Mix (PE Applied Biosystems, CA). The primer set applied to amplify La protein messenger RNA (mRNA) consisted of 5′-CGCTGGGAGGTGGAGTCGTT-3′ (exon 1) and 5′-CCCGTGGCAAATTGAAGTCG-3′ (exon 2). The probe, 5′-TGCCCTGGAGGCCAAAATCTGTCATC-3′ (exon 2), was designed to target an internal region between the forward and reverse primers. The primer set for PTB mRNA was 5′-AGCACGCCAAGCTGTCGCT-3′ (exon 8) and 5′-GGAACGGAAAGGCCGAAGG-3′ (exons 8–10). The probe was 5′-ACACACGCCCAGACCTGCCTTCCG-3′ (exon 8). The primer set for eIF3 p170 protein mRNA was 5′-CCGGAAAATGCCCTCAAACTA-3′ (exon 1) and 5′-AAGTGGCTCTTGCGAAGATCCACGC-3′ (exon 7). The probe sequence was 5′-CCAACGAATTTCTTGAGGTT-3′ (exon 2). The primer set for the internal control glyceraldehyde-3-phosphate dehydrogenase mRNA was designed according to GenBank M33197 by using the following primers: exon 7, 5′-TGCACCACCAACTGCTTAGCACCC-3′; and exon 8, 5′-CTTGATGTCATCATATTTGGCAGG-3′. The probe for glyceraldehyde-3-phosphate dehydrogenase-P, designed on the basis of exons 7 and 8, was 5′-TGACCACAGTCCATGCCATCACTGC-3′. Fifty PCR amplification cycles of 95°C for 30 seconds, 60°C for 40 seconds, and 72°C for 30 seconds were repeated by using a real-time PCR system (ABI PRISM 7700 Sequence Detection System; PE Applied Biosystems). To prepare standard RNA, PCR products were cloned into pBluescript vector and linearized at the T3 promoter site. Standard RNA was synthesized by using T7 RNA polymerase and purified by using Isogen (Wako Junyaku, Osaka, Japan) and deoxyribonuclease I (TaKaRa, Shiga, Japan). We detected HCV RNA in liver by using RTD-PCR as previously described.[38]

Statistical Analysis

All data are expressed as means ± SEM. Significance was tested by the Student *t* test and 1-way analysis of variance with Bonferroni's methods.

Results

Gene-Expression Profiling in Confluent or Serum-Starved Cells and the Activities of Hepatitis C Virus Internal Ribosomal Entry Site–Directed Translation

RCF-26 cell lines constitutively express dicistronic RNA transcripts containing sequences encoding the reporter proteins RL and FL separated by a functional HCV IRES (Figure 1). The activities of these proteins expressed in RCF-26 cells reflect cap-dependent and HCV IRES–directed translation, respectively. To rule out the possibility that FL activity from the second cistron reflected the nonspecific ribosomal scanning rather than HCV IRES–directed translation, we evaluated RL and FL activities in ΔRCF-9 cells in which the functional HCV IRES element had been deleted. The ratio of FL to RL (relative HCV IRES activity) in ΔRCF-9 was 2.5% of that in RCF-26, thus reflecting the specificity of HCV IRES activity in RCF-26 cells (Figure 2*B–D*). F2

To examine the relationship of the cellular proteins that vary in abundance and HCV IRES activities, RCF-26 cells and ΔRCF-9 cells were cultured in 15-cm dishes at confluence or under serum depletion for 48 hours, and changes in cellular gene expression and HCV IRES activities were evaluated. Under these conditions, the cellular DNA content increased at G_0/G_1 phase (49% to 74% in confluent cells and to 59% in serum-starved cells) and decreased at S phase (38% to 18% in confluent cells and to 35% in serum-starved cells) or G_2/M phase (14% to 8% in confluent cells and to 6% in serum-starved cells; Figure 2*A*). The degree of changes during the cell cycle was much greater in the confluent cells than in the serum-starved cells. The activities of HCV IRES–directed translation were reduced to 24% in confluent cells and to 22% in serum-starved cells compared with controls (Figure 2*C* and *D*), whereas the activities of cap-dependent cellular translation were essentially maintained (Figure 2*B*). Neither a significant difference in FL activity nor relative HCV IRES activity was found in ΔRCF-9 under these conditions (Figure 2*C* and *D*).

These results were not due to variations in the RNA stability of the RL and FL reporter genes. Northern blotting of mRNA transcribed from dicistronic constructs containing sequences encoding these 2 reporter proteins did not show either RNA degradation or splicing (data not shown). The relative expression ratio of mRNA of RL to FL determined by cDNA microarray did not change in either confluent or serum-starved cells (Figure 2*E*).

Gene-expression profiling changed in response to these conditions listed in Table 1. Serum proteins such as T1 α_2-macroglobulin and albumin, as well as cell adhesion molecules such as cadherin, major histocompatibility complex, and fibronectin, were up-regulated by more than 1.8-fold. Albumin, a major serum protein that is specifically produced in the liver, was remarkably regulated in a cell-cycle dependent manner. However, cell-cycle and growth-related genes such as cyclin A, cyclin B, CDK1, cell division cell cycle 18, p53, hepatoma-derived growth factor, and nm23 were down-regulated, as were genes related to RNA polymerase, such as RMP, La protein, and topoisomerase II. The La protein binds the stem loop IV structure in HCV IRES and stimulates HCV IRES–directed translation.[16,17] With regard to

tapraid2/zg0-gast/zg0-gast/zg000205/zg01756d05z | xppws | S=1 | 1/4/05 | Art: 51756 | DTD5.0

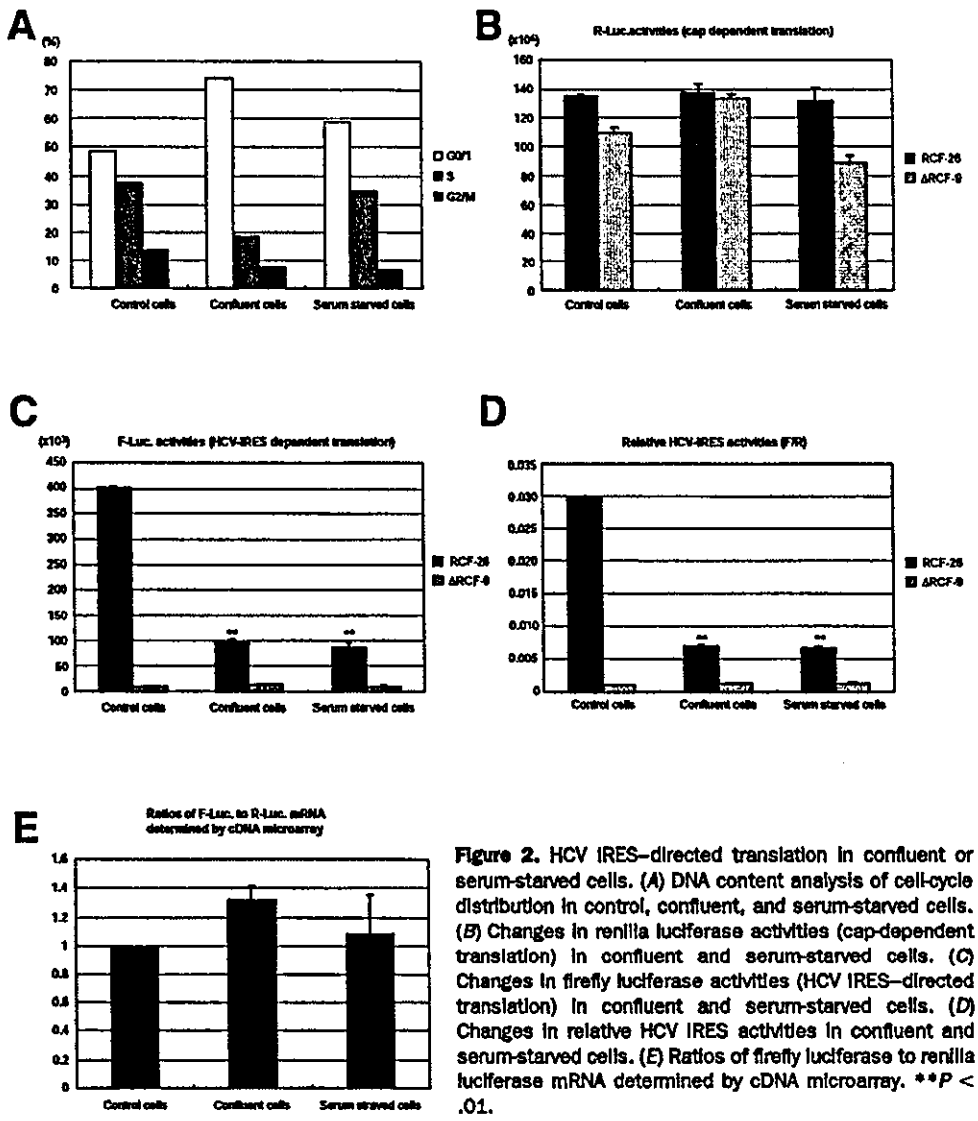

Figure 2. HCV IRES–directed translation in confluent or serum-starved cells. (*A*) DNA content analysis of cell-cycle distribution in control, confluent, and serum-starved cells. (*B*) Changes in renilla luciferase activities (cap-dependent translation) in confluent and serum-starved cells. (*C*) Changes in firefly luciferase activities (HCV IRES–directed translation) in confluent and serum-starved cells. (*D*) Changes in relative HCV IRES activities in confluent and serum-starved cells. (*E*) Ratios of firefly luciferase to renilla luciferase mRNA determined by cDNA microarray. $^{**}P < .01$.

changes in the expression of canonical and noncanonical initiation factors (Table 2), La protein and PTB expression were repressed in both confluent and serum-starved cells. The expression of eIF3 (p170 and p116) was predominantly repressed in confluent cells, and the expression of eIF2γ was predominantly repressed in serum-starved cells. Conversely, the expression of ribosomal protein S9 and PABPC-1 was induced in confluent cells. The degree to which gene expression changed was more predominant in confluent cells than in serum-starved cells. This might reflect the greater degree of changes in the cell-cycle distribution of G_0/G_1 and S phases in confluent cells than in serum-starved cells (Figure 2*A*). The results of northern blots of La protein, PTB, and albumin expression coincided with these results (Figure 3). We evaluated changes in La protein and PTB expression by using RTD-PCR. The relative expression of La protein in confluent and serum-starved cells was 16% and 33% of control cells, respectively. The relative expression of PTB in confluent and serum-starved cells was 10% and 26% of control cells, respectively (data not shown). These data suggest that several canonical and noncanonical initiation factors, such as La protein, PTB, eIF3, and eIF2γ, are initiation factors responsible for regulating HCV IRES activity in a cell cycle–dependent manner.

Hepatitis C Virus Internal Ribosomal Entry Site Activity at Different Phases of the Cell Cycle

We examined the relationship between HCV IRES activity and cell division in more detail. We

Table 1. Up- and Down-regulated Genes in Confluent and Serum-Starved Cells

UniGene	Gene name	Category	Confluent cells	Serum-starved cells	Mean
Up-regulated					>1.8
Hs.74561	Alpha-2-macroglobulin	Serum protein	12.87 ± 2.13	5.13 ± 0.10	9.00 ± 2.40
Hs.75442	Albumin	Serum protein	6.07 ± 1.07	3.26 ± 0.37	4.67 ± 0.93
Hs.77054	B-cell translocation gene 1	Antiproliferative gene	4.73 ± 1.76	2.97 ± 0.83	3.85 ± 0.94
Hs.82004	Cadherin 1, E-cadherin (epithelial)	Cell adhesion	5.14 ± 2.46	2.36 ± 0.30	3.75 ± 1.29
Hs.2257	Vitronectin	Cell adhesion	3.97 ± 0.68	2.11 ± 0.22	3.04 ± 0.61
Hs.277477	MHC class IC	Cell adhesion	3.26 ± 0.82	2.17 ± 0.09	2.71 ± 0.46
Hs.77961	MHC class IB	Cell adhesion	3.33 ± 0.23	2.08 ± 0.24	2.71 ± 0.39
Hs.1119	TR3 orphan receptor	Receptor	3.38 ± 1.23	1.95 ± 0.23	2.66 ± 0.66
Hs.1665	Zinc finger transcriptional regulator	Transcription factor	2.66 ± 0.40	2.53 ± 0.40	2.60 ± 0.23
Hs.287820	Fibronectin gene	Cell adhesion	2.40 ± 0.77	2.11 ± 0.34	2.26 ± 0.36
Hs.2780	JunD	Oncogene	2.23 ± 0.39	1.99 ± 0.54	2.11 ± 0.28
Down-regulated					<0.55
Hs.89525	Hepatoma-derived growth factor	Cell growth	0.67 ± 0.27	0.42 ± 0.08	0.55 ± 0.13
Hs.7943	RMP	RNA polymerase II binding	0.44 ± 0.09	0.64 ± 0.07	0.54 ± 0.07
Hs.23960	Cyclin B	Cell cycle	0.44 ± 0.25	0.62 ± 0.17	0.53 ± 0.13
Hs.118638	Nm23A	Cell growth	0.52 ± 0.01	0.53 ± 0.11	0.52 ± 0.05
Hs.83715	Autoantigen La	RNA polymerase III synthesis	0.43 ± 0.06	0.61 ± 0.01	0.52 ± 0.06
Hs.16297	COX17	Cytochrome-c-oxidase	0.47 ± 0.14	0.55 ± 0.06	0.51 ± 0.07
Hs.95577	CDK1	Cell cycle	0.36 ± 0.02	0.65 ± 0.07	0.50 ± 0.09
Hs.174017	Topoisomerase (DNA) II alpha	RNA polymerase II holoenzyme	0.44 ± 0.11	0.55 ± 0.08	0.50 ± 0.05
Hs.85137	Cyclin A	Cell cycle	0.42 ± 0.03	0.56 ± 0.17	0.49 ± 0.08
Hs.9235	Nucleoside-diphosphate kinase	Cell growth	0.51 ± 0.08	0.46 ± 0.05	0.49 ± 0.04
Hs.75133	Transcription factor 6–like 1	Transcription factor	0.40 ± 0.07	0.57 ± 0.18	0.48 ± 0.09
Hs.69563	Cell division cycle 18	Cell cycle	0.45 ± 0.04	0.51 ± 0.09	0.48 ± 0.04
Hs.58593	RAP30	Transcription factor	0.37 ± 0.02	0.58 ± 0.00	0.48 ± 0.06
Hs.75323	Prohibitin	Antiproliferative gene	0.50 ± 0.01	0.39 ± 0.01	0.44 ± 0.03
Hs.1846	p53	Cell cycle	0.66 ± 0.18	0.22 ± 0.04	0.44 ± 0.15
Hs.111758	Keratin 6	Housekeeping	0.24 ± 0.02	0.63 ± 0.07	0.43 ± 0.12
Hs.78271	Keratin 8	Housekeeping	0.33 ± 0.18	0.53 ± 0.08	0.43 ± 0.10
Hs.748	Fibroblast growth factor receptor 1	Cell growth	0.39 ± 0.12	0.30 ± 0.05	0.34 ± 0.06

synchronized cell-cycle progression and compared the production of RL and FL reporter proteins during different phases of the cell cycle. Cells were blocked at the G_1/S interface by adding aphidicolin to the culture medium and were then released from the aphidicolin block. Synchronized cells subsequently moved into the S and G_2/M phases of the cell cycle and then returned to G_1/S phase at approximately 27 hours, as deter-

Table 2. Up- and Down-regulated Initiation Factors in Confluent and Serum-Starved Cells

UniGene	Gene name	Confluent cells	Serum-starved cells	Mean
Hs.180920	Ribosomal protein S9	1.92 ± 0.01	1.11 ± 0.18	1.51 ± 0.24
Hs.172550	Polypyrimidine tract binding protein (PTB)	0.62 ± 0.17	0.62 ± 0.03	0.62 ± 0.07
Hs.83715	La protein	0.43 ± 0.06	0.61 ± 0.01	0.52 ± 0.06
Hs.2730	Heterogeneous nuclear ribonucleoprotein L (RNPL)	1.23 ± 0.33	1.02 ± 0.13	1.13 ± 0.16
Hs.63525	Poly(rC)-binding protein 2 (PCBP2)	1.20 ± 0.11	0.95 ± 0.10	1.07 ± 0.09
Hs.172182	Poly(A)-binding protein, cytoplasmic 1	1.87 ± 0.62	1.19 ± 0.05	1.53 ± 0.32
Hs.183418	Cell division cycle 2–like 1 (PITSLRE proteins)	0.85 ± 0.10	0.70 ± 0.07	0.78 ± 0.07
Hs.198899	eIF3-p170	0.47 ± 0.28	1.10 ± 0.36	0.79 ± 0.26
Hs.57783	eIF3-p116	0.58 ± 0.12	0.70 ± 0.02	0.64 ± 0.06
Hs.4310	eIF1A	0.84 ± 0.06	0.89 ± 0.17	0.86 ± 0.07
Hs.151777	eIF2A	1.37 ± 0.20	1.59 ± 0.20	1.48 ± 0.13
Hs.12163	eIF2β	0.88 ± 0.10	0.94 ± 0.02	0.91 ± 0.04
Hs.211539	eIF2γ	1.31 ± 0.03	0.61 ± 0.17	0.96 ± 0.22
Hs.129673	eIF4A	1.05 ± 0.09	0.81 ± 0.07	0.93 ± 0.08
Hs.93379	eIF4B	1.38 ± 0.48	0.94 ± 0.20	1.16 ± 0.25
Hs.79306	eIF4E	0.86 ± 0.14	0.83 ± 0.01	0.84 ± 0.06
Hs.286236	eIF5	0.91 ± 0.02	1.23 ± 0.35	1.07 ± 0.17

tapraid2/zg0-gast/zg0-gast/zg000205/zg01756d05z | xppws | S=1 | 1/4/05 | Art: 51756 | DTD5.0

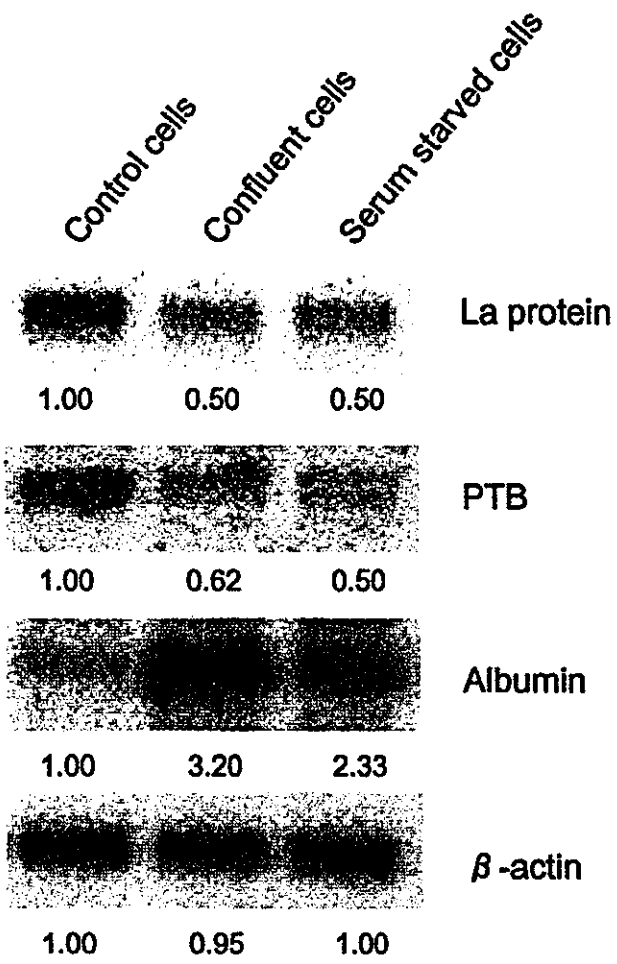

Figure 3. Northern blotting of La protein, PTB, and albumin in RCF-26. Expression of La protein and PTB is repressed in confluent and serum-starved cells, whereas albumin expression is significantly up-regulated.

mined by the cellular DNA content measured by flow cytometry (Figure 4*A*). RL activities increased proportionally, reflecting the increased number of cells after division. The cell number doubled at approximately 27 hours after 1 round of the cycle was completed. Conversely, HCV IRES activity varied with cell cycle, and the ratio of FL to RL (relative HCV IRES activity) increased during and immediately after G_2/M phase (12–18 hours after release from aphidicolin). The relative HCV IRES activity decreased by 36 hours after release (Figure 4*C*), corresponding to reentry into the G_0 and G_1 phases. However, the HCV IRES activity increased again, starting at approximately 39 hours, probably because many cells continued into a second cycle (Figure 4*A* and *C*). No significant differences in relative HCV IRES activity were found in ΔRCF-9 cells up to 30 hours after release (Figure 4*C*).

Gene-Expression Profiles in Cells Undergoing Cell-Cycle Progression

To determine which host factors are involved in this cell cycle–dependent regulation of HCV IRES activity, we evaluated gene-expression profiles in cells undergoing cell-cycle progression. Total RNA was extracted from synchronized cells at 3, 9, 15, 18, 24, 30, 36, and 42 hours after release from the aphidicolin block (G_1/S border) and was analyzed with the cDNA microar-

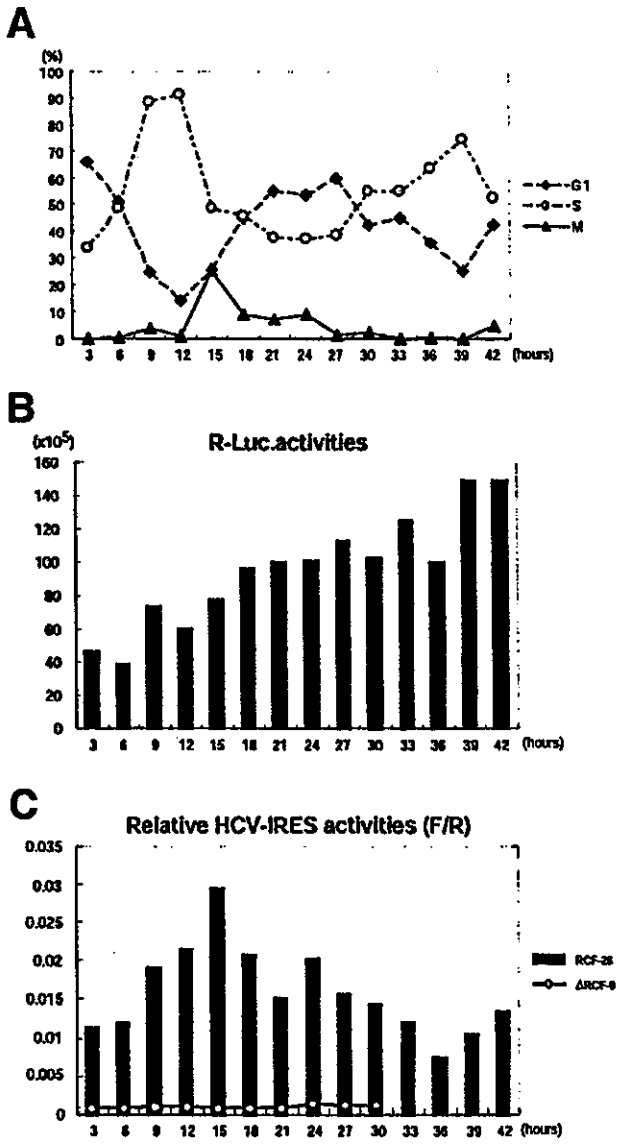

Figure 4. HCV IRES activity and cell-cycle progression. (*A*) Changes in distribution with cell-cycle progression. Proportions of G_1, S, and G_2/M are individually shown. (*B*) Changes of renilla luciferase activities (cap-dependent translation) with cell-cycle progression. (*C*) Changes in relative HCV IRES activities (firefly to renilla luciferase activities; FL/RL) with cell-cycle progression. HCV IRES activity varied with cell cycle in RCF-26 cells but did not change in ΔRCF-9 cells.

tapraid2/zg0-gast/zg0-gast/zg000205/zg01756d05z | xppws | S=1 | 1/4/05 | Art: 51756 | DTD5.0

ray. We constructed a 1-dimensional SOM to evaluate changes in gene expression (cluster and tree view; http://rana.Stanford.EDU/software/). We identified 3 large gene clusters as the cell cycle progressed. The first cluster of genes was induced at S phase (at 3 to 9 hours). The second and third clusters were induced at G_2/M (at 15–18 hours) and at G_1 (at 24 to 36 hours), respectively. Most of the HCV IRES–related canonical and noncanonical initiation factors were induced during S and G_2/M phases. PCBP-2, PTB, eIF3 (p110 and p170), eIF2γ, and eIF2β were induced during S phase, whereas La protein and RNPL were induced during G_2/M. These factors bind HCV IRES structure or have functional relevance to HCV IRES activity. Conversely, PABPC-1, eIF4A, and eIF4B were induced during G_1 phase. These factors are not required for HCV IRES–directed translation but are necessary for cap-dependent translation.[39] The induction of the ribosomal protein S9 in G_1 phase was a controversial finding because S9 was reported to bind stem loop IIId of HCV IRES. The functional role of the ribosomal protein S9 is discussed later. In cells, translation takes place immediately in the presence of mRNA, and luciferase activity could be detected within 30 seconds from the initiation of the translation. Thus, the induction of canonical and noncanonical initiation factors related to HCV IRES during S and G_2/M phases contributed to cell cycle–dependent regulation of translation directed by HCV IRES (Figure 5).

We evaluated changes in La protein expression determined by the cDNA microarray by using RTD-PCR (Figure 6). The changes in HCV IRES–directed translation and in La protein expression closely correlated (Figure 6).

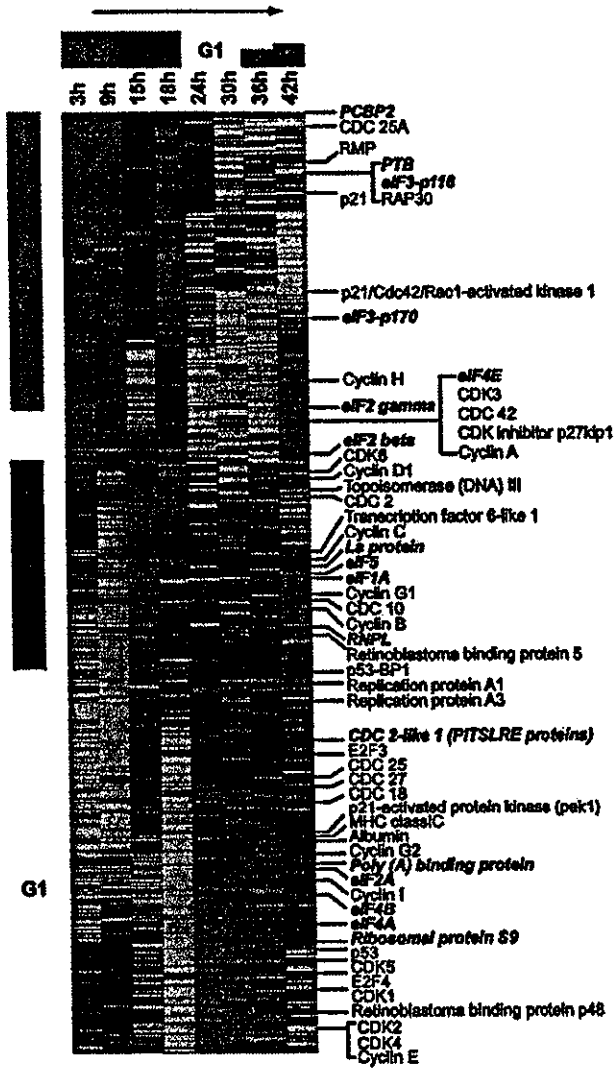

Figure 5. Gene-expression profiling in RCF-26 cells undergoing cell-cycle progression. RCF-26 cells were synchronized at the G_1/S border with aphidicolin. After release from aphidicolin block, the cell cycle progressed to S phase at 3–6 hours and G_2/M phase at 15–18 hours and returned to G_1 phase at 24–30 hours. Cells were harvested at 3, 9, 15, 18, 24, 30, 36, and 42 hours and analyzed with cDNA microarray, and then an SOM was constructed by using Cluster (Stanford University). Gene clusters up-regulated in the S, G_2/M, and G_1 phases (*red*) were detected with cell-cycle progression. Canonical and noncanonical initiation factors and cell cycle–related genes are listed (*right*).

Functional Analysis of the Effect of HCV IRES-Related Canonical and Noncanonical Initiation Factors on Translation Directed by HCV IRES

To prove that the induction of the canonical and noncanonical initiation factors during S and G_2/M phases contributes to cell cycle–dependent translation of HCV, antisense phosphorothioate oligos were designed for La protein, PTB, eIF3 p170, eIF2γ, RNPL, PABPC-1, PCBP-2, and ribosomal protein S9, and HCV IRES activity was evaluated under the suppression of these factors. RT-PCR showed that expression of the targeted factors was significantly reduced by the antisense oligos, whereas that of β-actin did not significantly change (Figure 7*B*). Reduced expression of these factors was also evaluated by Western blotting (Figure 7*C*). The suppression of La protein, PTB, and eIF2γ specifically reduced HCV IRES activity to 40%, 50%, and 53% of the control level, respectively. The effect of inhibiting HCV IRES activity was equal to or greater than that exerted by an antisense oligo against 5′-NTR of HCV (nt 330–350). However, suppression of eIF3 p170, RNPL, PABPC-1, PCBP-2, and ribosomal protein S9 did not reduce HCV IRES activity (Figure 7*A*). To rule out the possibility that these reduced HCV IRES activities were not due to nonspecific suppression by the antisense oligos, antisense oligos to La protein, PTB, eIF3 p170, and

COLOR

taprald2/zg0-gast/zg0-gast/zg000205/zg01756d05z | xppws | S=1 | 1/4/05 | Art: 51756 | DTD5.0

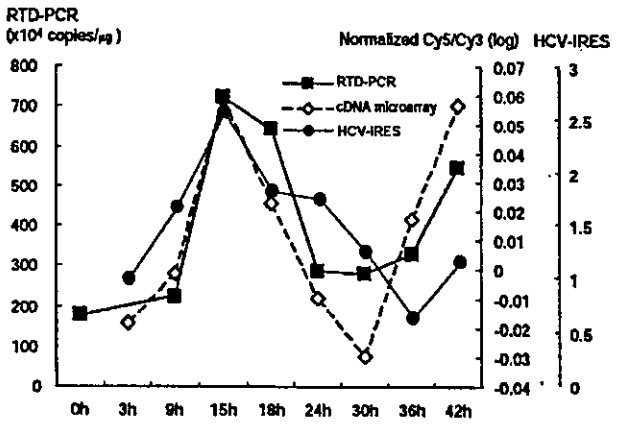

Figure 6. La protein expression in RCF-26 under cell-cycle progression determined by RTD-PCR. Normalized Cy5/Cy3 of mRNA expression of La protein and HCV IRES activities are shown in same dimension.

ribosomal protein S9 were applied to ΔRCF-9 in which the functional HCV IRES element had been deleted. Two antisense oligos to La protein and PTB, which reduced HCV IRES activity in RCF-26, did not change HCV IRES activity in ΔRCF-9. Similarly, 2 antisense oligos to eIF3 p170 and ribosomal protein S9, which had no effect on HCV IRES activity, did not have any effect on HCV IRES activity in ΔRCF-9 (Figure 7*A*). Conversely, overexpression of La protein, PTB, and eIF3 p170 significantly enhanced HCV IRES activity in a dose-dependent manner, whereas the overexpression of eIF2γ, RNPL, PCBP-1, PCBP-2, and ribosomal protein S9 had no effect (Figure 8). The overexpression of La protein, PTB, and eIF3 p170 in ΔRCF-9 did not have any effect on HCV IRES activity (Figure 8). We also confirmed these findings in rabbit reticulocyte lysates by co-translating pRL-HL (HCV IRES reporter) and La protein, PTB, and eIF3 p170 (data not shown). Thus, of these HCV IRES–related canonical and noncanonical initiation factors, La protein and PTB significantly changed HCV IRES activity in both the suppressed and overexpressed states. Thus, changes in the expression of these factors alter HCV IRES activity in a cell cycle–dependent manner.

Expression of La Protein, Polypyrimidine Tract Binding Protein, and Eukaryotic Initiation Factor 3 in Lesions of Chronic Hepatitis C

To examine the functional role of these factors on HCV replication in the lesions of chronic hepatitis C, we evaluated their expression in 26 liver samples from patients with chronic hepatitis C and in 8 normal liver samples by RTD-PCR. Tables 3 and 4 list the clinical characteristics of the patients. The expression level of La protein in the specimens of the patients with chronic hepatitis C was significantly higher than that of the normal livers, whereas the expression of PTB and eIF3 p170 was not statistically different (Table 3). Some of these samples were also reevaluated by Northern blotting, and the results were similar (data not shown). Up-regulation of the La protein was related to neither the histological stage nor the activity of liver disease (Table 4). However, the expression of La protein was significantly correlated with the amount of HCV RNA in the liver (Figure 9). Moreover, HCV RNA replication was significantly higher in liver with high La protein expression (Figure 10). These findings indicate that La protein plays an important role in the replication of HCV in the livers of patients infected with chronic hepatitis C.

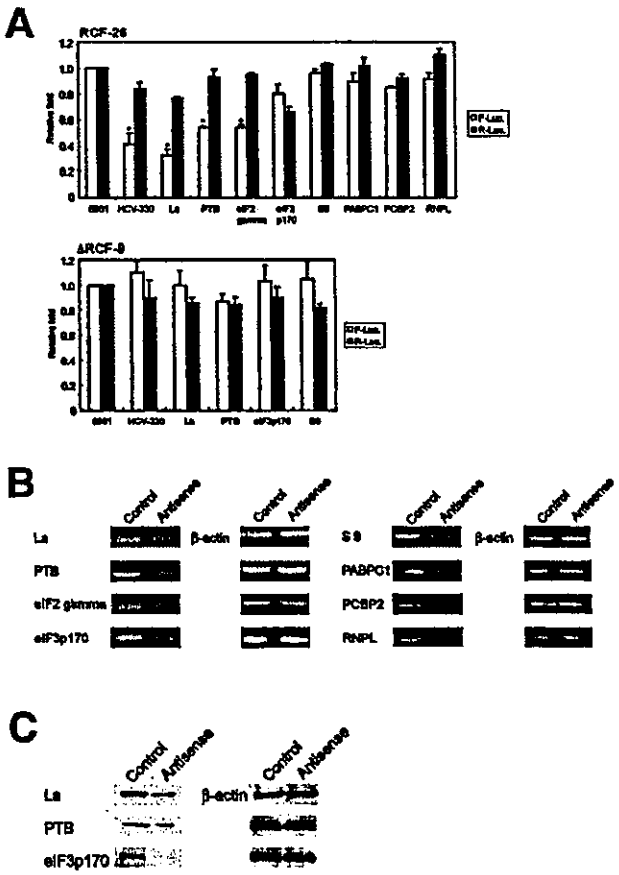

Figure 7. Suppression of HCV IRES–related canonical and noncanonical initiation factors (La protein, PTB, eIF3 [p170], eIF2γ, RNPL, PABPC-1, PCBP-2, and ribosomal protein S9) by specific antisense phosphorothioate oligos and HCV IRES activity in RCF-26 and ΔRCF-9. (*A*) Changes in renilla (cap-dependent translation) and firefly luciferase (HCV IRES–directed translation) activities caused by suppression of these factors by antisense phosphorothioate oligos. $*P < .05$. (*B*) Suppression of factors confirmed by RT-PCR. (*C*) Suppression of factors confirmed by Western blotting.